J|A|C|S
ARTICLES
Published on Web 02/14/2003

Mechanistic Studies of Nickel(II) Alkyl Agostic Cations and Alkyl Ethylene Complexes: Investigations of Chain Propagation and Isomerization in (α-diimine)Ni(II)-Catalyzed Ethylene Polymerization

Mark D. Leatherman, Steven A. Svejda, Lynda K. Johnson, and Maurice Brookhart*

Contribution from the Department of Chemistry, University of North Carolina at Chapel Hill, CB# 3290 Venable Hall, Chapel Hill, North Carolina 27599-3290

Received August 12, 2002; E-mail: mbrookhart@unc.edu

Abstract: The synthesis of a series of (α-diimine)NiR_2 (R = Et, ^{n}Pr) complexes via Grignard alkylation of the corresponding (α-diimine)$NiBr_2$ precursors is presented. Protonation of these species by the oxonium acid $[H(OEt_2)_2]^+[BAr'_4]^-$ at low temperatures yields cationic Ni(II) β-agostic alkyl complexes which model relevant intermediates present in nickel-catalyzed olefin polymerization reactions. The highly dynamic nature of these agostic alkyl cations is quantitatively addressed using NMR line broadening techniques. Trapping of these complexes with ethylene provides cationic Ni alkyl ethylene species, which are used to determine rates of ethylene insertion into primary and secondary carbon centers. The Ni agostic alkyl cations are also trapped by CH_3CN and Me_2S to yield $Ni(R)(L)^+$ (L = CH_3CN, Me_2S) complexes, and the dynamic behavior of these species in the presence of varied [L] is discussed. The kinetic data obtained from these experiments are used to present an overall picture of the ethylene polymerization mechanism for (α-diimine)-Ni catalysts, including effects of reaction temperature and ethylene pressure on catalyst activity, polyethylene branching, and polymer architecture. Detailed comparisons of these systems to the previously presented analogous palladium catalysts are made.

Introduction

Significant recent research has been directed toward the design and application of catalyst systems based on late transition metals capable of effecting the polymerization of olefins to high molar mass homo- and copolymers.[1−12] Reports from these laboratories[13,14] and DuPont[15−19] have explored Ni-(II)- and Pd(II)-α-diimine systems that exhibit several unique features, including the copolymerization of ethylene and functionalized olefins,[20−23] the oligomerization of ethylene and α-olefins,[24−26] the living polymerization of ethylene and α-olefins,[27,28] and the homopolymerization of cyclic[16] and internal acyclic olefins.[29]

The microstructure of polyethylene produced by nickel(II)- and palladium(II)-diimine catalysts varies from strictly linear

(1) Keim, W.; Appel, R.; Storeck, A.; Kruger, C.; Goddard, R. *Angew. Chem., Int. Ed. Engl.* **1981**, *20*, 116−117.
(2) Möhring, V. M.; Fink, G. *Angew. Chem., Int. Ed. Engl.* **1985**, *24*, 1001−1003.
(3) Ostoja Starzewski, K. A.; Witte, J. *Angew. Chem.* **1985**, *97*, 610−612.
(4) Klabunde, U.; Ittel, S. D. *J. Mol. Catal.* **1987**, *41*, 123−134.
(5) Brookhart, M.; DeSimone, J. M.; Grant, B. E.; Tanner, M. J. *Macromolecules* **1995**, *28*, 5378−5380.
(6) Small, B. L.; Brookhart, M.; Bennett, A. M. A. *J. Am. Chem. Soc.* **1998**, *120*, 4049−4050.
(7) Small, B. L.; Brookhart, M. *Macromolecules* **1999**, *32*, 2120−2130.
(8) Britovsek, G. J. P.; Gibson, V. C.; Kimberly, B. S.; Maddox, P. J.; McTravish, S. J.; Solan, G. A.; White, A. J. P.; Williams, D. J. *Chem. Commun.* **1998**, 849−850.
(9) Britovsek, G. J. P.; Gibson, V. C.; Wass, D. F. *Angew. Chem., Int. Ed.* **1999**, *38*, 429−447.
(10) Younkin, T. R.; Connor, E. F.; Henderson, J. I.; Friedrich, S. K.; Grubbs, R. H.; Bansleben, D. A. *Science* **2000**, *287*, 460−462.
(11) Hicks, F. A.; Brookhart, M. *Organometallics* **2001**, *20*, 3217−3219.
(12) Ittel, S. D.; Johnson, L. K.; Brookhart, M. *Chem. Rev.* **2000**, *100*, 1169−1203.
(13) Johnson, L. K.; Killian, C. M.; Brookhart, M. *J. Am. Chem. Soc.* **1995**, *117*, 6414−6415.
(14) Gates, D. P.; Svejda, S. A.; Oñate, E.; Killian, C. M.; Johnson, L. K.; White, P. S.; Brookhart, M. *Macromolecules* **2000**, *33*, 2320−2334.
(15) Brookhart, M. S.; Johnson, L. K.; Killian, C. M.; Arthur, S. D.; Feldman, J.; McCord, E. F.; McLain, S. J.; Kreutzer, K. A.; Bennett, A. M. A.; Coughlin, E. B.; Ittel, S. D.; Parthasarathy, A.; Tempel, D. J. WO Patent Application 9623010 to DuPont, April 3, 1995.
(16) McLain, S. J.; Feldman, J.; McCord, E. F.; Gardner, K. H.; Teasley, M. F.; Coughlin, E. B.; Sweetman, K. J.; Johnson, L. K.; Brookhart, M. *Macromolecules* **1998**, *31*, 6705−6707.
(17) Guan, Z.; Cotts, P. M.; McCord, E. F.; McLain, S. J. *Science* **1999**, *283*, 2059−2062.
(18) Cotts, P. M.; Guan, Z.; McCord, E. F.; McLain, S. J. *Macromolecules* **2000**, *33*, 6945−6952.
(19) McCord, E. F.; McLain, S. J.; Nelson, L. T. J.; Arthur, S. D.; Coughlin, E. B.; Ittel, S. D.; Johnson, L. K.; Tempel, D. J.; Killian, C. M.; Brookhart, M. *Macromolecules* **2001**, *34*, 362−371.
(20) Johnson, L. K.; Mecking, S.; Brookhart, M. *J. Am. Chem. Soc.* **1996**, *118*, 267−268.
(21) Mecking, S.; Johnson, L. K.; Wang, L.; Brookhart, M. *J. Am. Chem. Soc.* **1998**, *120*, 888−899.
(22) Johnson, L.; Bennett, A.; Dobbs, K.; Hauptman, E.; Ionkin, A.; Ittel, S.; McCord, E.; McLain, S.; Radzewich, C.; Yin, Z.; Wang, L.; Wang, Y.; Brookhart, M. *Polym. Mater. Sci. Eng.* **2002**, *86*, 319.
(23) McLain, S. J.; Sweetman, K. J.; Johnson, L. K.; McCord, E. F. *Polym. Mater. Sci. Eng.* **2002**, *86*, 320−321.
(24) Killian, C. M.; Johnson, L. K.; Brookhart, M. *Organometallics* **1997**, *16*, 2005−2007.
(25) Tempel, D. J. Ph.D. Dissertation, University of North Carolina at Chapel Hill, 1998.
(26) Svejda, S. A.; Brookhart, M. *Organometallics* **1999**, *18*, 65−74.
(27) Killian, C. M.; Tempel, D. J.; Johnson, L. K.; Brookhart, M. *J. Am. Chem. Soc.* **1996**, *118*, 11664−11665.
(28) Gottfried, A. C.; Brookhart, M. *Macromolecules* **2001**, *34*, 1140−1142.
(29) Leatherman, M. D.; Brookhart, M. *Macromolecules* **2001**, *34*, 2748−2750.

10.1021/ja021071w CCC: $25.00

Scheme 1. Proposed Mechanism of Ethylene Polymerization

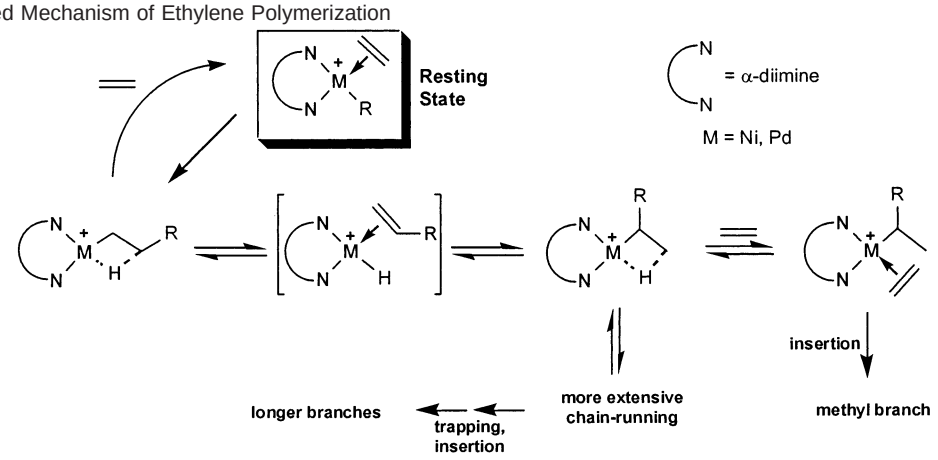

to highly branched, while the microstructures of poly(α-olefins) produced by these same catalyst systems are characterized by fewer branches than are expected from 1,2-monomer enchainment (chain-straightening).[13,14] The degree of branching in the polyethylene and the polymer architecture can depend on a number of factors: the metal, the steric bulk of the diimine ligand, and the reaction conditions. Polyethylenes produced by palladium(II)-diimine catalysts are generally highly branched (e.g., >70 methyls/1000 carbons) regardless of ligand structure or reaction conditions, although the precise polymer architecture varies from linear polyethylene with short chain branches, obtained at high ethylene pressures, to a more hyperbranched structure at lower ethylene concentrations.[17] In contrast, polyethylenes prepared from nickel(II)-diimine catalysts display overall branching numbers that are quite variable. Polymerizations run at low temperatures and high ethylene pressure using nickel complexes bearing relatively nonbulky diimine ligands yield nearly linear polyethylene, while higher temperatures and/or lower ethylene concentrations in combination with nickel complexes bearing sterically demanding diimine ligands result in more highly branched polyethylene.[12−14,30] In the case of nickel-catalyzed polymerization of α-olefins, the degree of chain-straightening observed in the resulting poly(α-olefin)s is strongly affected by diimine ligand symmetry and reaction conditions.[25] Palladium catalysts generally produce more chain-straightened poly(α-olefin) products than their nickel analogues, but unlike the nickel systems, the degree of branching seen in poly(α-olefin)s produced by the palladium complexes is relatively independent of ligand structure and reaction conditions.

Mechanistic studies of ethylene polymerizations catalyzed by both nickel(II)- and palladium(II)-diimine complexes have led to the proposed polymerization mechanism shown in Scheme 1.[13,25,31−35] Following initiation, the mechanism is characterized by chain propagation, chain isomerization, and chain transfer steps. To date, the chain propagation step is the best-studied portion of the overall mechanism. Low-temperature NMR studies of ethylene polymerization have established the catalyst

Scheme 2. Isomerization Equilibria in (α-diimine)Pd Complexes

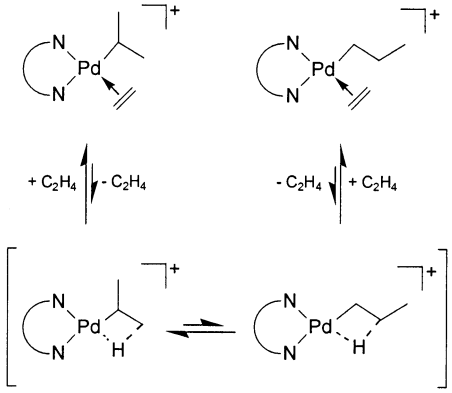

resting state for both metals under these conditions as the alkyl ethylene complexes, implying turnover-limiting migratory insertion of ethylene. Activation barriers to ethylene insertion have been measured for both palladium and nickel complexes. As previously reported, the activation barriers to ethylene insertion in the chain propagation step are 4−5 kcal/mol lower for the nickel complexes as compared to their palladium congeners.[32]

Mechanistic studies of the chain isomerization process have focused on (α-diimine)Pd(II) complexes. As established by these studies, alkyl chain isomerization occurs in the β-agostic species, which can be formed either after olefin insertion from the metal(alkyl)olefin resting state or by ethylene loss from the resting state. The barrier to interconversion of the resulting β-agostic species (via β-H elimination, olefin rotation, and reinsertion) is quite low (<11 kcal/mol), and the rate of the interconversion is much faster than the rate of trapping of the β-agostic species by ethylene. Low-temperature NMR studies of these (α-diimine)Pd(II) β-agostic complexes have further established that the activation barriers to olefin insertion (propagation) are ca. 17−18 kcal/mol and are *significantly higher* than the activation barriers for chain isomerizations occurring from these resting states.[25,33,34] This feature is illustrated in the simplified version of chain isomerization shown in Scheme 2. Low-temperature NMR studies have shown that the (α-diimine)Pd(^{i}Pr)$(C_2H_4)^+$ and (α-diimine)Pd(^{n}Pr)$(C_2H_4)^+$ complexes *completely equilibrate* via ethylene loss and isomerization of the agostic species *prior* to insertion. That chain isomerization occurs rapidly relative to insertion even from the catalyst resting state explains both the highly branched polyethylenes produced by the (α-diimine)palladium systems and the independence of the total

(30) Killian, C. M. Ph.D. Dissertation, University of North Carolina at Chapel Hill, 1996.
(31) Tempel, D. J.; Brookhart, M. *Organometallics* **1998**, *17*, 2290−2296.
(32) Svejda, S. A.; Johnson, L. K.; Brookhart, M. *J. Am. Chem. Soc.* **1999**, *121*, 10634−10635.
(33) Tempel, D. J.; Johnson, L. K.; Huff, R. L.; White, P. S.; Brookhart, M. *J. Am. Chem. Soc.* **2000**, *122*, 6686−6700.
(34) Shultz, L. H.; Tempel, D. J.; Brookhart, M. *J. Am. Chem. Soc.* **2001**, *123*, 11539−11555.
(35) Shultz, L. H.; Brookhart, M. *Organometallics* **2001**, *20*, 3975−3982.

Scheme 3. Synthesis of Pd β-Agostic Isopropyl Complexes

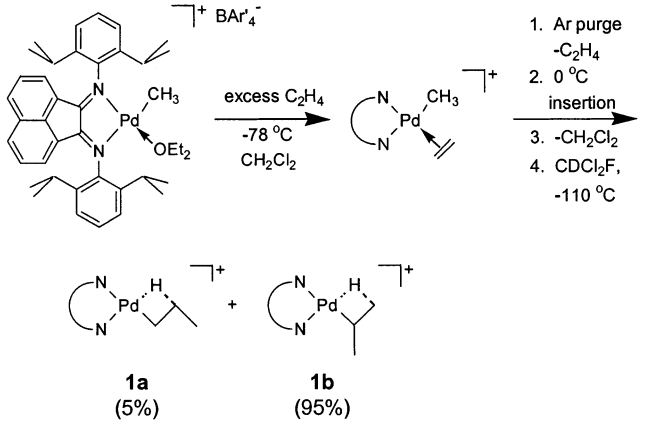

degree of polymer branching on ethylene pressure demonstrated by palladium catalysts. However, since the rate of trapping is first-order in ethylene, the average distance that the Pd center "walks" along the polymer chain prior to insertion is affected by monomer concentration, resulting in varying polymer topologies depending on olefin pressure.[17]

Thus far, the mechanism of chain growth and chain isomerization has been studied in some detail for the palladium systems. In contrast, difficult synthesis and manipulation of well-defined (α-diimine)nickel(II) complexes has, until recently, hindered mechanistic investigations of these systems. However, recent advances in the preparation and purification of such complexes have facilitated mechanistic studies of olefin insertion and chain growth processes in these systems.[32] In this paper, an account of our studies of cationic (α-diimine)Ni(II) β-agostic complexes is presented. Some implications of these studies concerning the mechanism of chain isomerization during (α-diimine)nickel(II)-catalyzed olefin polymerizations are discussed and compared to Pd(II) analogues.

Results

A. Synthesis and Reactivity of (α-Diimine)Ni(II) β-Agostic *n*-Propyl and Isopropyl Complexes. Recent work in our laboratory with (α-diimine)Pd(II) β-agostic complexes has established that chain isomerization occurs rapidly relative to chain propagation.[25,33,34] In these experiments, palladium β-agostic complexes **1a** and **1b** were prepared and isolated on a preparative scale using the conditions shown in Scheme 3. Since the barrier to ethylene insertion is relatively high in these palladium complexes, the clean, quantitative formation of the methyl ethylene complex shown in Scheme 3 is straightforward. Excess monomer can be easily purged from the solution with argon. Migratory insertion of ethylene occurs when the solution is warmed to 0 °C. The isopropyl β-agostic complex **1b** is the observed reaction product, which presumably forms following rapid isomerization of the initially formed *n*-propyl β-agostic complex **1a**. When the solution is cooled to −110 °C, the agostic hydrogens of complexes **1a** and **1b** are clearly observed in the ^{1}H NMR spectra.

Attempts to form β-agostic nickel complexes through insertion of 1 equiv of ethylene in nickel methyl ethylene complexes were unsuccessful (Scheme 4). The addition of 1 equiv of ethylene to ether adduct **2** at −110 °C led to very slow formation of methyl ethylene complex **3**. Even at −110 °C, multiple insertions of ethylene occurred prior to complete ether displacement, resulting in a complex mixture of the starting ether adduct, the desired methyl ethylene compound **3**, and various insertion products. Use of a large excess of ethylene to hasten the formation of the methyl ethylene complex **3** from ether adduct **2**, followed by an argon purge to remove the excess ethylene, also failed. Multiple insertions of ethylene again occurred, possibly due to slight warming of the solution by the argon purge gas. The sterically bulkier diisopropyl ether ligand of $[(ArN{=}C(An){-}C(An){=}NAr)Ni(CH_3)(O^iPr_2)]^+[BAr_4']^-$ (Ar = 2,6-$C_6H_3Me_2$), **4**, was anticipated to undergo more facile displacement by ethylene to form methyl ethylene complex **3**. Unfortunately, numerous attempts to prepare **4** failed to yield the desired product; this compound appears to be unstable even at −78 °C.

An alternative route to the desired β-agostic nickel complexes based upon protonolysis of an (α-diimine)$NiPr_2$ complex with $[H(OEt_2)_2]^+[BAr'_4]^-$ was found to be successful. Alkylation of (α-diimine)$NiBr_2$ complexes **5** and **6** with 2 equiv of *n*-propylmagnesium bromide in diethyl ether at −78 °C produced the corresponding (α-diimine)$NiPr_2$ complexes **7** and **8** (Scheme 5). Use of ethylmagnesium bromide in this synthesis produces the corresponding (α-diimine)$NiEt_2$ complexes **9** and **10** (Scheme 5). Diethyl ether solutions of all complexes are very dark blue in color, while the complexes are dark purple in the solid state. The solids appear to be stable indefinitely when stored at temperatures below −15 °C in a drybox, but are thermally sensitive in solution. Complexes **7**, **8** and **9**, **10** undergo reductive elimination to yield hexane or butane, respectively,

Scheme 4. Attempted Synthesis of Ni β-Agostic Complexes through Single Ethylene Insertion

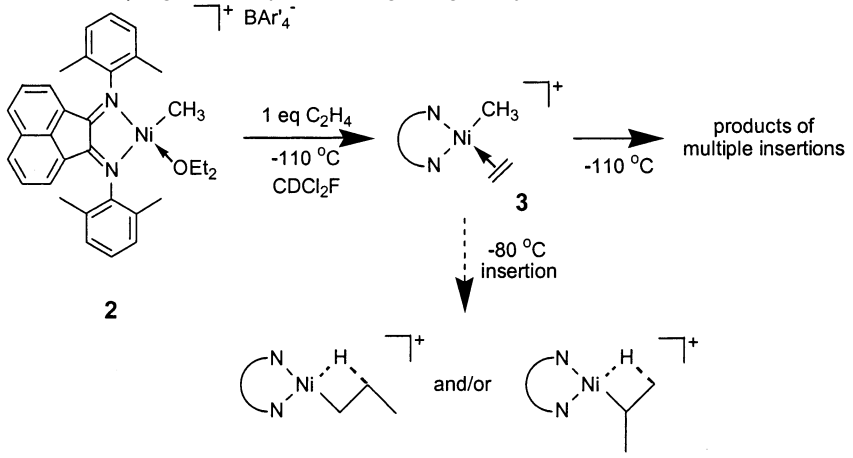

Scheme 5. Synthesis of (α-diimine)Nickel Di-*n*-propyl and Diethyl Complexes

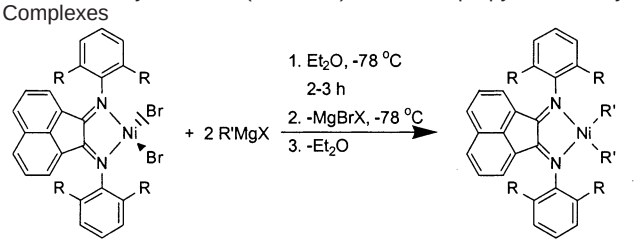

5 R = Me
6 R = ^{i}Pr

7 R = Me, R' = ^{n}Pr
8 R = ^{i}Pr, R' = ^{n}Pr
9 R = Me, R' = Et
10 R = ^{i}Pr, R' = Et

Scheme 6. Synthesis of Ni β-Agostic Complexes ***i*-11**/***n*-11** via Protonolysis of Nickel Dipropyl Complex **7**

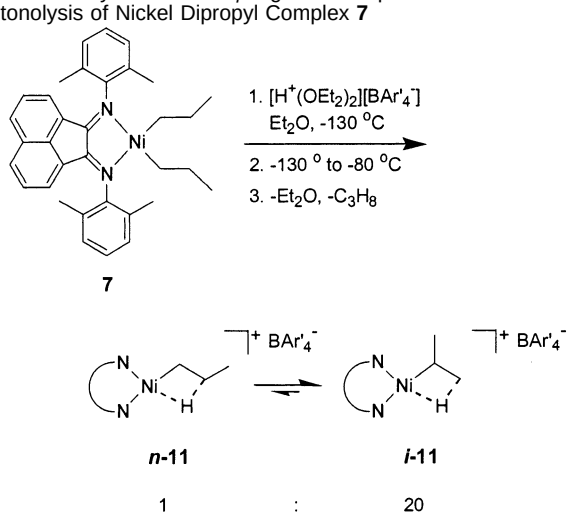

7

***n*-11** : **20** ***i*-11**

1

when their CD_2Cl_2 solutions are warmed above −20 °C. These complexes are extremely air-sensitive and immediately decompose to form unknown products when exposed to the air. Reactions of the nickel diethyl complexes **9** and **10** will be discussed in the following section.

Protonolysis of nickel dipropyl complex **7** with 1 equiv of $[H(OEt_2)_2]^+[BAr'_4]^-$ in diethyl ether at approximately −100 °C yields propane and a mixture of two β-agostic species (Scheme 6). The mixture consists of a 20:1 equilibrium ratio of β-agostic isopropyl complex ***i*-11** and β-agostic *n*-propyl complex ***n*-11**. DFT calculations are in agreement with the observed relative stabilities of ***i*-11** and ***n*-11** and suggest that the origin of the difference is electronic rather than steric in nature.[36,37] The *n*-propyl complex ***n*-11** is presumably the initial product formed immediately following the loss of propane after protonation of **7**. Complex ***n*-11** then isomerizes to the β-agostic isopropyl complex ***i*-11**. The structure of the β-agostic isopropyl complex ***i*-11** was confirmed by low-temperature NMR experiments (^{1}H and ^{1}H−^{1}H COSY) obtained in $CDCl_2F$ at −130 °C. The proton NMR resonance of the β-agostic hydrogen of ***i*-11** is observed as a triplet (δ −12.5, $^2J_{HH}$ = 19 Hz), while the β-agostic hydrogen of the *n*-propyl complex ***n*-11** appears as a doublet (δ −13.0, $^2J_{HH}$ = 19 Hz) (see Supporting Information for the ^{1}H NMR spectrum of the agostic region). The other two hydrogens on the agostic methyl group (complex ***i*-11**) are

(36) Musaev, D. G.; Froese, R. D. J.; Svensson, M.; Morokuma, K. *J. Am. Chem. Soc.* **1997**, *119*, 367−374.
(37) Deng, L.; Woo, T. K.; Cavallo, L.; Margl, P. M.; Ziegler, T. *J. Am. Chem. Soc.* **1997**, *119*, 6177−6186.

Scheme 7. Dynamic Processes Observed in β-Agostic Isopropyl Complex ***i*-11**

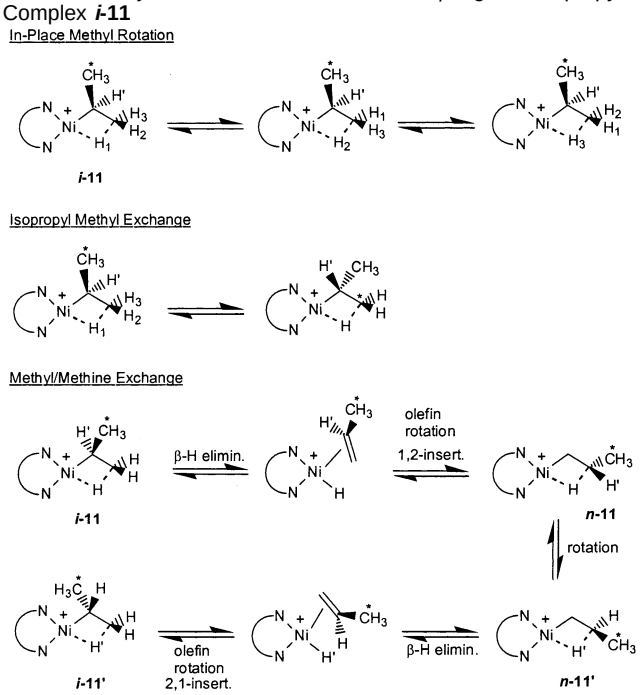

chemically inequivalent and appear as broad multiplets at 0.26 and 0.11 ppm. The nonagostic methyl group resonance appears as a broad singlet at −0.09 ppm. The resonance due to the isopropyl methine hydrogen (δ 2.00) is a complex multiplet at temperatures below −120 °C, but appears as a septet at temperatures above −80 °C.

Variable-temperature ^{1}H NMR studies reveal that three distinct dynamic processes occur in complex ***i*-11**: in-place methyl rotation, isopropyl methyl exchange, and methyl/methine hydrogen exchange. These processes are shown in Scheme 7. Two of these processes, in-place methyl rotation and isopropyl methyl exchange, are relatively low-energy processes as compared to methyl/methine hydrogen exchange. As previously mentioned, at temperatures below −120 °C, the proton NMR resonance of the β-agostic hydrogen of complex ***i*-11** is observed as a triplet. Above −120 °C this signal quickly broadens, as do the agostic and, at slightly higher temperatures, the nonagostic isopropyl methyl resonances. This dynamic behavior is indicative of facile hydrogen exchange through an in-place rotation of the agostic methyl group, along with exchange of the agostic methyl group with the free methyl group via rotation of the isopropyl group about the Ni−C bond (Scheme 7).[31] Quantitative dynamic NMR spectroscopic analysis allows for the determination of the energy barriers for these processes. Using the slow exchange approximation, in-place methyl rotation occurs with a $\Delta G^{\ddagger}$ of 8.0 kcal/mol at −99 °C, and the barrier to isopropyl methyl exchange is slightly higher, 9.0 kcal/mol at −77 °C. Coalescence of these six protons is observed as a broad resonance at δ −2.1 ppm at temperatures above −50 °C. Over the temperature range of −140 to −40 °C, the isopropyl methine resonance displays no discernible line broadening; only above −30 °C does this resonance begin to broaden. These observations indicate that the barrier to exchange of the isopropyl methine hydrogen with the isopropyl methyl hydrogens (interconversion of ***i*-11** and ***i*-11′**, Scheme 7) is considerably higher than the barriers to in-place methyl rotation and

isopropyl methyl exchange. Line broadening analysis establishes a $\Delta G^{\ddagger}$ of ca. 13.9 kcal/mol at 5 °C for this process. The overall dynamic behavior exhibited by this agostic nickel complex is similar to that reported for the analogous, well-studied β-agostic isopropyl palladium complex.[31] In the Pd case, the barrier to β-H elimination/reinsertion (measured for the Pd ethyl agostic cation as 6.8 kcal/mol at −120 °C)[38] is lower than the barrier for either in-place rotation (9.1 kcal/mol at −90 °C) or methyl exchange (9.6 kcal/mol at −90 °C), indicating that the β-H elimination is likely not the rate-determining step in the chain isomerization. In contrast, the comparatively large $\Delta G^{\ddagger}$ for scrambling of the methine hydrogen in ***i*-11** supports the β-H elimination/reinsertion step as rate-determining for the Ni system (additional evidence for this supposition comes from study of the agostic ethyl complex, presented in the following section).

Ligand steric effects on the dynamic processes in nickel propyl agostic cations were examined using the Ni(^{i}Pr) agostic complex **12** [(ArN═C(An)−C(An)═NAr)Ni(CH(CH$_2$-μ-H)-(CH$_3$))]$^+$[BAr$_4$′]$^-$ (Ar = 2,6-C$_6$H$_3$^{i}Pr$_2$), obtained via protonolysis of **8** as previously described. This reaction furnishes the isopropyl agostic species exclusively, as no characteristic resonances for the *n*-propyl group are observed in the agostic or alkyl regions of the low-temperature static ^{1}H NMR spectrum (−120 °C, CDCl$_2$F).[39] The agostic resonance for this complex again appears as a triplet (δ −12.5, $^2J_{HH}$ = 18 Hz). ^{1}H−^{1}H COSY experiments allow assignment of the two nonagostic methyl protons of the agostic methyl group (δ 0.67, br m), the methine proton (δ 2.16, m), and the nonagostic methyl group (δ −0.22, br d). Complex **12** displays variable-temperature dynamic behavior similar to ***i*-11**, including scrambling of the three protons of the agostic methyl group ($\Delta G^{\ddagger}$ = 8.4 kcal/mol at −90 °C) and Ni−C$_\alpha$ bond rotation to equilibrate all six methyl protons ($\Delta G^{\ddagger}$ = 9.4 kcal/mol at −75 °C). The methine resonance is a sharp septet ($^2J_{HH}$ = 5.2 Hz) above −70 °C and broadens due to β-H elimination/reinsertion above −10 °C ($\Delta G^{\ddagger}$ = 13.4 kcal/mol). Comparison of these barriers to those determined for ***i*-11** shows that increased steric bulk around the metal center slightly increases the barriers to C$_\alpha$−C$_\beta$ and Ni−C$_\alpha$ bond rotations while slightly decreasing the β-H elimination/reinsertion rate.

When ca. 7 equiv of diethyl ether relative to complex ***i*-11** is present in a CDCl$_2$F NMR solution, new resonances in the proton NMR spectrum are observed. At −130 °C, previously unobserved peaks appear at 6.28 ppm (br), 3.95 ppm (br m), and 0.24 ppm (d, J = 6.7 Hz). These signals are consistent with a diethyl ether adduct. The resonance appearing at 6.28 ppm is due to the acenaphthene backbone *ortho* hydrogens, the resonance at 3.95 ppm is likely a methylene resonance of bound diethyl ether, and the doublet at 0.24 ppm is consistent with the isopropyl methyl group (eq 1). The equilibrium shown in eq 1 lies in favor of the β-agostic isopropyl complex ***i*-11**, as no diethyl ether adduct is observed when only 1 equiv of free ether is present. With 7 equiv of diethyl ether present, a roughly 1:1 ratio of the β-agostic isopropyl complex/diethyl ether adduct is observed (K_{eq} ca. 0.15 M^{-1}).

Scheme 8. Trapping of β-Agostic Species ***i*-11**/***n*-11** with Ethylene at −130 °C

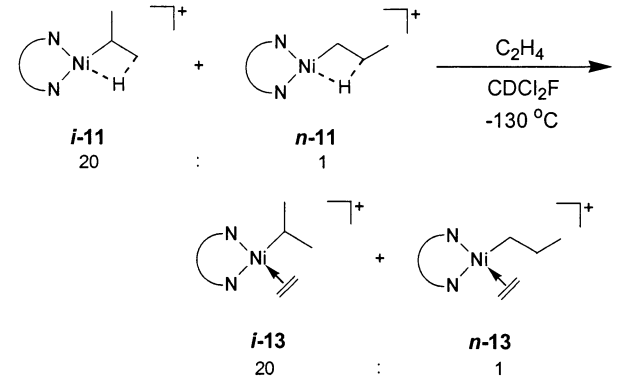

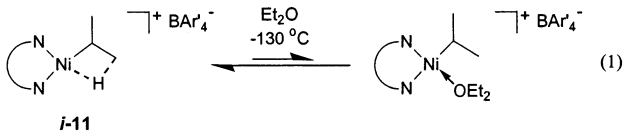

(1)

The addition of 5 equiv of ethylene at −130 °C to the mixture of β-agostic complexes ***i*-11** and ***n*-11** (produced in situ by protonolysis of nickel dipropyl complex **7**) results in trapping of the agostic complexes as their corresponding alkyl ethylene complexes ***i*-13** and ***n*-13** in a 20:1 ratio (Scheme 8). The structure of each complex was confirmed by low-temperature ^{1}H NMR and ^{1}H−^{1}H COSY NMR spectroscopy. Key ^{1}H NMR resonances for ***i*-13** (CDCl$_2$F/CDClF$_2$, −130 °C) include bound ethylene signals at 3.96 and 3.53 ppm (apparent d, 2H each), the isopropyl methine resonance at 1.47 ppm (m, 1H), and the isopropyl methyl resonance at 0.40 ppm (br s, 6H). Diagnostic resonances for ***n*-13** (CDCl$_2$F/CDClF$_2$, −100 °C) include the bound ethylene resonances at 4.17 and 3.31 ppm (br d, 2H each) and the *n*-propyl group resonances at 1.22 ppm (m, 2H, NiCH$_2$C*H*$_2$CH$_3$), 0.61 ppm (t, J = 6.9 Hz, 3H, NiCH$_2$CH$_2$C*H*$_3$), and 0.48 ppm (t, J = 7.5 Hz, 2H, NiC*H*$_2$CH$_2$CH$_3$). At −130 °C, no insertion of ethylene into the Ni−alkyl bond of either complex is observed.

When the protonolysis of nickel dipropyl complex **7** with 1 equiv of [H(OEt$_2$)$_2$]$^+$[BAr′$_4$]$^-$ is carried out in the presence of ethylene at −130 °C, the *n*-propyl ethylene complex ***n*-13** is the only product observed (Scheme 9). This result supports the initial formation of the β-agostic *n*-propyl complex ***n*-11** immediately following protonolysis. In the absence of a trapping ligand such as ethylene, the β-agostic *n*-propyl complex ***n*-11** isomerizes to the β-agostic isopropyl complex ***i*-11**. In the presence of ethylene, the initially formed β-agostic *n*-propyl complex ***n*-11** is trapped by ethylene faster than it isomerizes via β-elimination/readdition, forming ***n*-13**. Isomerization of ***n*-13** to ***i*-13** is not observed at temperatures between −130 and −90 °C, characterized by the lack of the distinctive isopropyl methyl doublet upfield of all other Ni-alkyl resonances. However, ethylene insertion does occur at −100 °C, and subsequent chain growth to give the linear alkyl species **14** is observed (Scheme 9).

At temperatures above −100 °C, migratory insertion of ethylene in complex ***i*-13** is observed (Scheme 10). As the

(38) In the ^{1}H NMR spectra, the resonance for the methine hydrogen in the Pd(isopropyl)agostic complex is obscured by ligand resonances; thus quantitative analysis of its dynamic behavior cannot be determined. Therefore, the barrier obtained in the similar Pd ethyl agostic species is used as an approximation in this analysis.

(39) Calculations predict the ^{i}Pr agostic complex to be thermodynamically favored even in the presence of bulky ligands: Deng, L.; Woo, T. K.; Cavallo, L.; Margl, P. M.; Ziegler, T. *J. Am. Chem. Soc.* **1997**, *119*, 6177−6186. A small amount of the ^{n}Pr agostic analogue of **12** may be present upon protonolysis of **8** (as seen in ***i*-11**/***n*-11**) with obscured resonances in the ^{1}H NMR spectrum.

Scheme 9. Protonolysis of **7** in the Presence of 5 equiv of C_2H_4 at −130 °C and Subsequent Reactivity of *n*-Propyl Ethylene Complex ***n*-13**

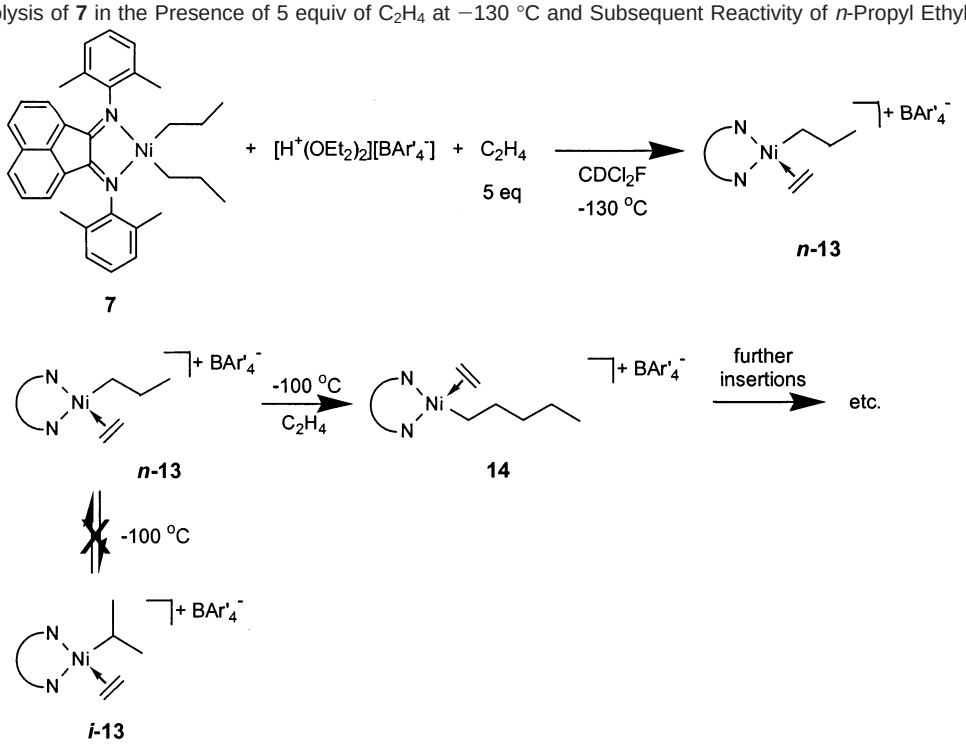

Scheme 10. Ethylene Insertion into the Ni−Isopropyl Bond of Complex ***i*-13**

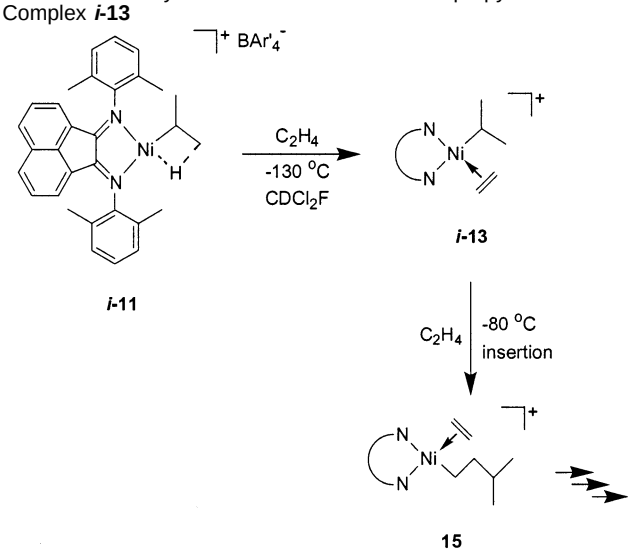

isopropyl methyl ^{1}H NMR resonance disappears (δ 0.39, d, J = 5.9 Hz, −80 °C), new resonances appear at δ 0.96 (br m, −80 °C) and δ 0.64 (d, J = 6.1 Hz, −80 °C), which are consistent with the isopropyl methine and methyl groups, respectively, of the single insertion product **15** (Scheme 10). Isomerization of ***i*-13** to ***n*-13** prior to the initial ethylene insertion *does not* occur, since none of the characteristic resonances for ***n*-13** or its single insertion product are observed. Also, the appearance of the previously unobserved doublet at 0.64 ppm and resonances corresponding to the α- and β-methylene protons of **15** (δ 0.47, t, J = 6.4 Hz and 1.07, br q, J = 6.4 Hz) with the coincidental disappearance of the isopropyl methyl doublet in ***i*-13** strongly suggests that migratory insertion of ethylene into the Ni-2° alkyl bond of ***i*-13** is occurring much faster than isomerization of ***i*-13** to ***n*-13**. The ethylene insertion barriers in both ***i*-13** and ***n*-13** are discussed below.

Studies of similar Pd alkyl ethylene complexes have established that Pd *n*-propyl ethylene and Pd isopropyl ethylene complexes equilibrate prior to insertion via reversible ethylene loss and facile β-elimination/reinsertion.[25,33] Attempts to probe the possible existence and nature of such an equilibrium between the analogous Ni complexes ***i*-13** and ***n*-13** have shown no observable ethylene dissociation or alkyl chain isomerization in ***i*-13** up to −80 °C, but are complicated by the relatively low barrier to olefin insertion. However, the use of small, nucleophilic, noninserting ligands such as acetonitrile and dimethyl sulfide to trap the free agostic alkyl cation provides insight into the alkyl chain isomerization behavior of these complexes. Introduction of a solution of 2 equiv of $NCCH_3$ in CD_2Cl_2 to a solution of ***i*-11**/***n*-11** (20:1) in CD_2Cl_2 in an NMR tube at −80 °C furnishes the Ni(isopropyl)($NCCH_3$) complex ***i*-16** and Ni(*n*-propyl)($NCCH_3$) complex ***n*-16** in a 20:1 kinetic ratio (consistent with the equilibrium ratio of ***i*-11**:***n*-11**) and 1 equiv of free $NCCH_3$ (Scheme 11). This ratio is unchanged upon warming the sample to temperatures up to −10 °C; at higher temperatures ***i*-16** isomerizes slowly to ***n*-16**, until an equilibrium mixture is reached (K_{eq} = 3, see Scheme 11). The dependence of this isomerization rate on ligand concentration was determined,[40] and the results are shown in Table 1. An approximately inverse dependence of isomerization rate on [$NCCH_3$] was observed over a 5-fold concentration range. This behavior shows that isomerization occurs via reversible dissociation of CH_3CN from ***i*-16** followed by rate-determining isomerization of ***i*-11** to ***n*-11** and rapid trapping by CH_3CN to yield ***n*-16**. A free energy diagram illustrating this process is shown in Figure 1. Similar effects are observed using dimethyl sulfide as the trapping ligand. Addition of 1 equiv of Me_2S to an NMR sample of ***i*-11**/***n*-11** at −80 °C yields a mixture of ***i*-17** and ***n*-17** (***n***-

(40) Espenson, J. H. *Chemical Kinetics and Reaction Mechanisms*; McGraw-Hill: New York, 1981.

Scheme 11. Isomerization Processes in Ni(propyl)(L) Cations (L = $NCCH_3$, SMe_2)

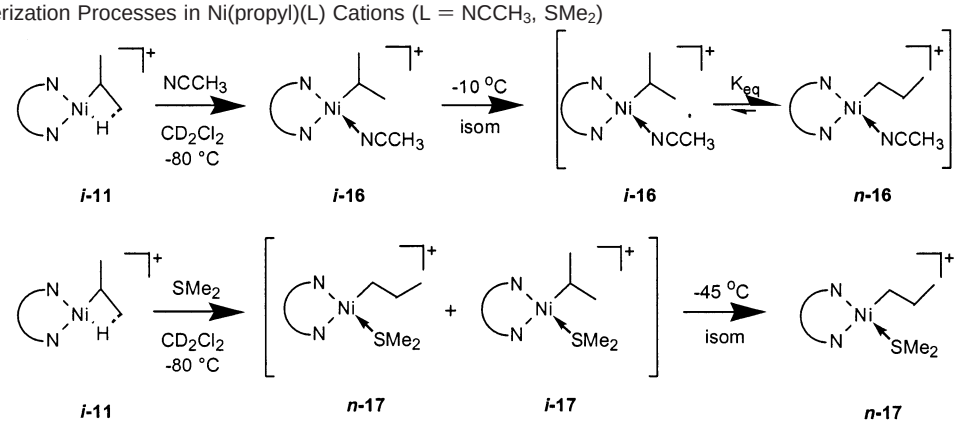

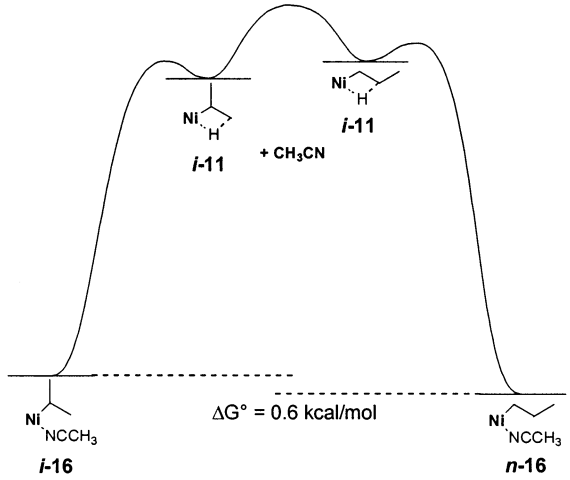

Figure 1. Free energy diagram for the isomerization of ***i*-16** to ***n*-16**

Table 1. Isomerization Rates of Ni(isopropyl)L Complexes ***i*-16** and ***i*-17**

Complex	[Ni-L] (M)	[excess L] (M)	k_1 (s^{-1})
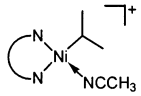	0.014	0.014	2.3×10^{-4} (-6.1 °C)
	0.015	0.036	7.4×10^{-5} (-6.3 °C)
	0.014	0.071	5.4×10^{-5} (-5.7 °C)
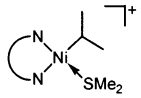	0.011	0	4.2×10^{-4} (-45.8 °C)
	0.010	0.044	1.8×10^{-4} (-45.8 °C)
	0.012	0.098	1.4×10^{-4} (-45.5 °C)

17/***i*-17** = 0.33), which begins to isomerize at −50 °C (Scheme 11). Complete conversion to the linear species ***n*-17** is observed. The isomerization rate of the dimethyl sulfide complex is also inhibited by excess ligand, but significant deviation from an inverse relationship between k_{isom} and [SMe_2] is observed (see last two entries in Table 1).[41]

B. (α-Diimine)Ni(II) *β*-Agostic Ethyl Complexes. The dynamics of the *β*-agostic isopropyl complex ***i*-8** discussed above shed some light on basic processes that occur during chain isomerization reactions of (α-diimine)Ni complexes. The anticipated dynamic behavior of the similar *β*-agostic ethyl complexes **18** and **19** would provide additional insight into the mechanism of chain isomerization. Spencer and co-workers have examined ligand substituent effects on dynamic processes in similar bisphosphine platinum[42,43] and nickel and palladium[44] ethyl agostic cations, including the isolation and X-ray structural characterization of a [(dbpe)Ni(C_2H_5)][BF_4] (dbpe = bis(di-*tert*-butylphosphino)ethane) complex. Rapid $C_\alpha-C_\beta$ bond rotation averages the agostic methyl hydrogens above −100 °C, but *β*-H elimination/reinsertion to equilibrate the two carbons and five protons is not observed below 27 °C.

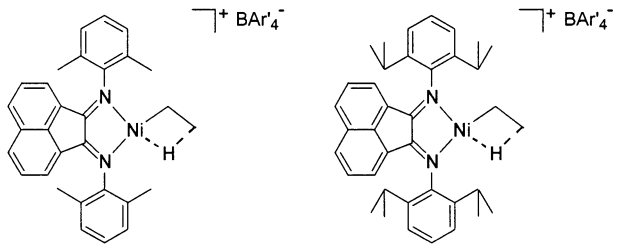

18 **19**

As mentioned in the previous section, protonolysis of nickel dipropyl complex **7** with $[H(OEt_2)_2]^+[BAr'_4]^-$ (Scheme 6) proved to be a convenient synthetic route to the *β*-agostic isopropyl complex ***i*-11**. Using the same strategy, protonolysis of nickel diethyl complex **9** with $[H(OEt_2)_2]^+[BAr'_4]^-$ was considered the best approach to the synthesis of *β*-agostic ethyl complex **18**. The synthesis of **9** was described in the previous section and is shown in Scheme 5. The combination of **9** and $[H(OEt_2)_2]^+[BAr'_4]^-$ at −130 °C in $CDCl_2F$ resulted in no immediate reaction, as determined by ^1H NMR. The sample was slowly warmed, and no appreciable protonation was observed until the temperature reached −90 °C. At −90 °C, the resonances of nickel diethyl complex **9** slowly disappeared, and at least two new nickel complexes were observed. The major compound present in this solution is the cationic nickel ethyl diethyl ether adduct **20** (Scheme 12). A $^1H-^1H$ COSY NMR

(41) This deviation suggests a mechanistic regime in which the barrier to trapping of ***i*-11** is comparable to the isomerization barrier (***i*-11** to ***n*-11**), and thus the loss of SMe_2 cannot be treated as fast and reversible relative to the isomerization step. The much lower temperature of isomerization of the SMe_2 complex and trapping of ***i*-11**/***n*-11** by SMe_2 in a nonkinetic ratio supports this contention.

(42) Carr, N.; Mole, L.; Orpen, A. G.; Spencer, J. L. *J. Chem. Soc., Dalton Trans.* **1992**, 2653−2662.
(43) Mole, L.; Spencer, J. L.; Carr, N.; Orpen, A. G. *Organometallics* **1991**, *10*, 49−52.
(44) Conroy-Lewis, F. M.; Mole, L.; Redhouse, A. D.; Litster, S. A.; Spencer, J. L. *J. Chem. Soc., Chem. Commun.* **1991**, 1601−1603.

Scheme 12. Protonation of Nickel Diethyl Complex **9** with $[H(OEt_2)_2]^+[BAr'_4]^-$

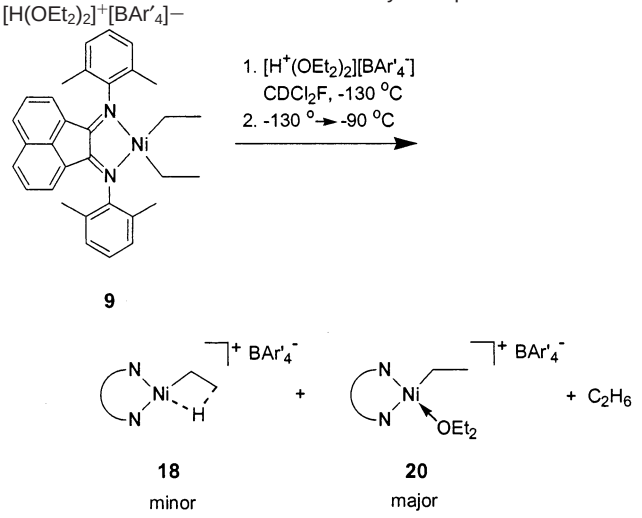

spectrum taken at −100 °C indicated that the Ni ethyl resonances for complex **20** appear at 1.23 (m) and −0.21 ppm (t). With respect to the minor species, no agostic resonance was observed (−12 to −14 ppm), but the $^1H-^1H$ COSY NMR spectrum revealed a correlation between a broad resonance at 1.56 ppm (tentatively NiCH_2) and a multiplet at 0.18 ppm (agostic methyl), consistent with **18**. A more definitive identification of diethyl ether coordination to a similar cationic palladium ethyl species has recently been obtained.[35]

Recent work with palladium analogues of **18** have revealed that diethyl ether competes with the agostic hydrogen for the vacant metal coordination site. However, substitution of sterically bulkier diisopropyl ether for diethyl ether resulted in clean formation of the palladium β-agostic ethyl complex, with no evidence for a palladium ethyl diisopropyl ether complex. Using this same approach, formation of the ether adduct can also be suppressed in the nickel systems. Substitution of $[H(O^iPr_2)_2]^+[BAr'_4]^-$ for $[H(OEt_2)_2]^+[BAr'_4]^-$ under the synthetic conditions shown in Scheme 12 results in the formation of **18** as the major reaction product. The agostic hydrogen for complex **18** appears at −13.7 ppm (br t, $J \approx 20$ Hz, $CDCl_2F$, −120 °C) in the ^1H NMR spectrum and is coupled to the two nonagostic protons of the methyl group at 0.39 ppm and weakly to the two methylene protons at 1.28 ppm. Some of the diethyl ether adduct **20** was also observed. Complete removal of diethyl ether from complex **9** has proven difficult due to the extreme thermal sensitivity of **9**. Therefore, the diethyl ether adduct **20** presumably forms as a consequence of the residual diethyl ether competing with the agostic hydrogen for the vacant coordination site.

Two distinct fluxional processes in **18** can be quantified using dynamic NMR analysis. At temperatures above −100 °C, the resonances of the agostic and nonagostic methyl protons begin to broaden, indicating facile rotation about the $C_\alpha-C_\beta$ bond and scrambling of the three protons. The barrier for this process was determined based on broadening of both resonances for the agostic and nonagostic protons, and both sets of data provide $\Delta G^\ddagger = 8.7$ kcal/mol at −85 °C. At more elevated temperatures (ca. −40 °C), the resonances for the three C_β protons coalesce at ca. δ −3.0 ppm. This resonance sharpens with increasing temperature, then begins to broaden at 10 °C due to exchange with the protons on C_α. Quantification of the broadening of the C_α protons provides a barrier of 14.0 kcal/mol at 6 °C for the β-hydride elimination−olefin rotation−reinsertion process.

As is the case for the Ni(propyl) agostic systems, ligand steric effects can be ascertained through the synthesis of Ni diethyl complex **10** (Scheme 5) and the analogous agostic cation **19**. Complex **10** was obtained with minor residual diethyl ether present (<0.25 equiv) and, upon protonation with $[H(O^iPr_2)_2]^+[BAr'_4]^-$, furnishes exclusively the ethyl agostic cation **19** in situ. The lack of diethyl ether coordination to the nickel center in this case is likely due to steric effects of the bulkier *ortho*-isopropyl groups on the ligand aryl rings. At −130 °C in $CDCl_2F$, **19** is not fluxional and exhibits distinct resonances for the two nonagostic protons of the methyl group (δ 0.35, m) and the agostic proton (δ −13.8, t, $J = 19$ Hz). The Ni−CH_2 resonances at 1.43 ppm were identified by significant coupling to the nonagostic methyl protons and weaker coupling to the agostic proton in the $^1H-^1H$ COSY spectrum, but were not observed directly due to the coincident shift of one of the ligand isopropyl methyl groups. As observed in complex **18**, the resonances of the agostic and nonagostic methyl protons of **19** begin to broaden above −105 °C and provide a $\Delta G^\ddagger = 8.6$ kcal/mol at −90 °C for the $C_\alpha-C_\beta$ bond rotation. Coalescence of these resonances is again observed (δ −4.2 ppm) at temperatures above −45 °C, followed by broadening due to exchange of all five ethyl protons through β-H elimination and reinsertion. However, since the resonance for the C_α protons is obscured by the methyl resonances of the ligand isopropyl groups, no quantitative analysis was feasible. An approximation for the β-H elimination−rotation−reinsertion process in **19** can be obtained from the broad coalesced methyl resonance at −4.2 ppm, which agrees with the barrier determined in **18** (ca. 14.3 kcal/mol at 30 °C in **19** vs 14.0 ± 0.1 kcal/mol at 6.4 °C in **18**).

C. Ethylene Insertion in (α-diimine)Ni(II) β-Agostic Propyl and Ethyl Complexes. Ethylene insertion into the cationic $(ArN{=}C(An)-C(An){=}NAr)Ni(CH_3)(C_2H_4)^+$ complexes **3** (Ar = 2,6-$C_6H_3(Me)_2$) and **21** (Ar = 2,6-$C_6H_3(^iPr)_2$) provides a convenient method for determination of the energy barriers for insertion into Ni-Me species as well as subsequent ethylene insertion.[32] The latter barrier is (theoretically) a weighted average of all ethylene insertions possible during the polymerization (e.g., insertion into Ni-1° C, 2° C, and 3° C bonds). However, the accessibility of the agostic complexes and ethylene-trapped species described in the previous sections allows measurement of the individual insertion barriers for each specific case with both ligands to give a more complete analysis of the relative energies of insertion versus isomerization.

As shown in Scheme 10, the (2,6-Me_2)Ar(α-diimine)Ni(*n*-propyl)ethylene complex ***n*-13**, generated by protonation of the dipropyl complex in the presence of ethylene, exhibits migratory insertion without observable isomerization at temperatures above −100 °C. The energy barrier for this process was determined to be 13.4 kcal/mol at −92 °C. Isopropyl ethylene complex ***i*-13** undergoes ethylene insertion with a barrier of 14.2 kcal/mol at −82 °C. Thus, there is a distinct difference between barriers to ethylene insertion into a primary and secondary carbon center. Comparisons to previously determined barriers will be addressed in the following section.

Migratory insertion rates for complexes with the more sterically demanding (2,6-^{i}Pr)Ar(α-diimine) ligand were determined in a similar fashion. However, the agostic ethyl complex

Scheme 13. Generation and Subsequent Insertion of Ni(ethyl)ethylene Cation **22** and Ni(isopropyl)ethylene Cation **23**

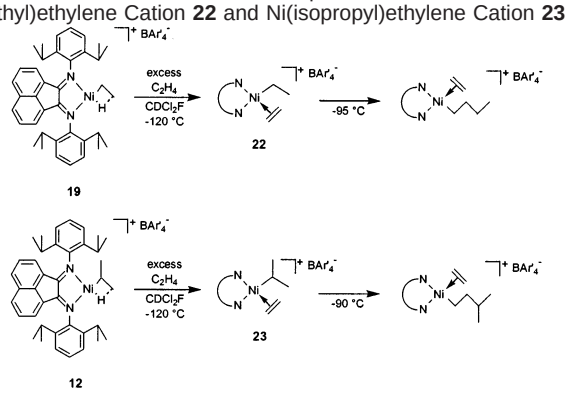

Table 2. Migratory Insertion Barriers of Ni Alkyl Ethylene Complexes[a]

complex	*k* (temp, °C)	$\Delta G^{\ddagger}$, kcal/mol
3	1.2×10^{-3} s^{-1} (−80.9)	13.6
***n*-13**	2.3×10^{-4} s^{-1} (−92.2)	13.4
***i*-13**	2.5×10^{-4} s^{-1} (−81.6)	14.2
21	3.1×10^{-4} s^{-1} (−92.9)	13.3
22	7.6×10^{-4} s^{-1} (−93.5)	12.9
23	2.2×10^{-4} s^{-1} (−88.5)	13.7

[a] Errors in $\Delta G^{\ddagger}$ measurements are ±0.1 kcal/mol (see Experimental Section).

19 was employed for measurement of olefin insertion into a primary carbon since it does not exhibit ether binding, which could be competitive with association of ethylene. This complex also precludes any complications due to alkyl isomerization prior to olefin insertion. Introduction of 5 equiv of C_2H_4 to a sample of **19** generated in situ in an NMR tube at −130 °C yields the Ni(ethyl)ethylene cation **22** quantitatively (Scheme 13). The characteristic alkyl resonances are observed at 0.85 ppm for the methylene protons and 0.65 ppm for the terminal methyl group. Olefin insertion in this species occurs with a $\Delta G^{\ddagger}$ of 12.9 kcal/mol at −94 °C. As in the previous case for the *ortho*-methyl ligand, treatment of the Ni(isopropyl) agostic cation **12** with excess ethylene at −130 °C generates the Ni(isopropyl)-ethylene complex **23**. This species exhibits behavior similar to ***i*-13** in that no isomerization to the linear alkyl-ethylene cation is observed prior to insertion, and this insertion barrier ($\Delta G^{\ddagger}$ = 13.7 kcal/mol at −89 °C) is significantly greater than that for the linear species.

Discussion

The mechanistic studies described here for (α-diimine)Ni catalysts, coupled with previous mechanistic studies of the Pd analogues, provide a quantitative comparison of the dynamics and reactivity of key intermediates in the ethylene polymerization reactions. The mechanistic data account for the differing rates of chain propagation and polymer microstructures observed for the two systems. The discussion below highlights the key differences between the Pd and Ni systems.

Insertion Barriers. Ethylene insertion barriers for the nickel alkyl ethylene complexes are 4−5 kcal/mol lower than their palladium congeners, accounting for the significantly greater turnover frequency observed in the nickel systems. With a barrier difference of 4−5 kcal/mol, turnover frequencies of Ni systems should be ca. 10^4 times greater than turnover frequencies for Pd analogues at 25 °C. This is in line with bulk polymerization results.[13]

Scheme 14. Generic Model for Metal Migration (Chain Walking)

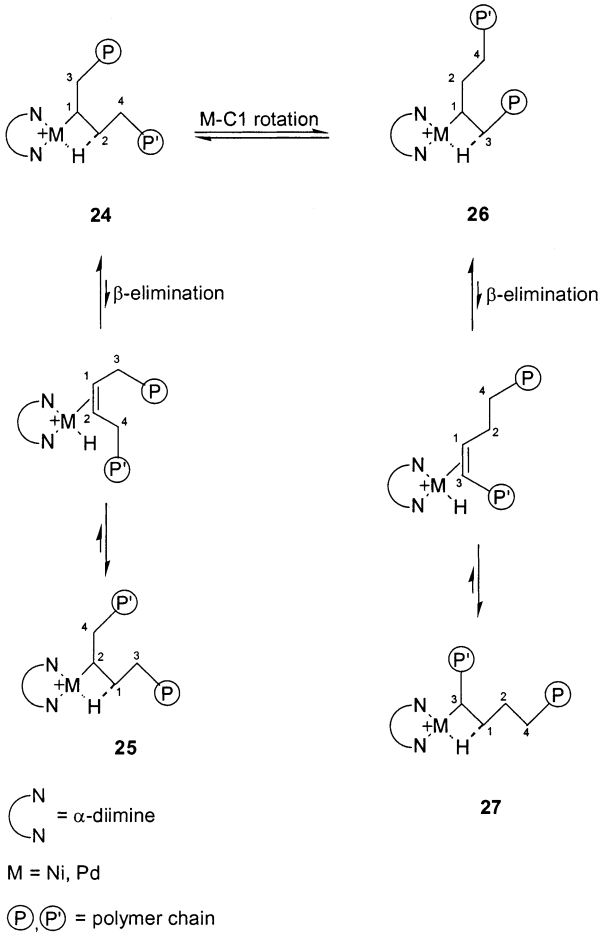

The influence of the ligand structure and the nature of the migrating alkyl group on insertion barriers can be discerned from the data summarized in Table 2. The primary alkyl groups (*n*-propyl for ***n*-13** and ethyl for **22**) exhibit barriers ca. 0.8 kcal/mol less than the corresponding barriers for the migration of the secondary isopropyl group (compare ***n*-13** to ***i*-13** and **22** to **23**). Ethylene insertion barriers for the bulkier diisopropyl(aryl)-substituted complexes **22** and **23** are ca. 0.5 kcal/mol lower than their dimethyl(aryl) counterparts ***n*-13** and ***i*-13** for insertions into both primary and secondary carbon centers. The lower barriers for the diisopropyl(aryl)-substituted systems account for the somewhat higher activity of these more hindered catalysts. These same trends are evident for the Pd complexes and are best rationalized by proposing that the steric interactions in the alkyl olefin ground states are more severe than in the transition states where the Ni−alkyl bond is lengthened, and thus the ground-state/transition-state energy difference is less for the bulkier diisopropyl(aryl)-substituted systems. Theoretical calculations have fairly accurately modeled the insertion barriers in these systems and the observed substituent effects.[36,37,45,46]

Metal Migration along the Polyethylene Chain (Chain Walking). Migration of the metal along the alkyl chain occurs by the processes shown in Scheme 14. The metal can move between C1 and C2 (**24** to **25**) via β-elimination and readdition.[47]

(45) Deng, L.; Margl, P. M.; Ziegler, T. *J. Am. Chem. Soc.* **1997**, *119*, 1094−1100.
(46) Froese, R. D. J.; Musaev, D. G.; Morokuma, K. *J. Am. Chem. Soc.* **1998**, *120*, 1581−1587.

Scheme 15. Mechanism for Formation of Branched Polyethylenes

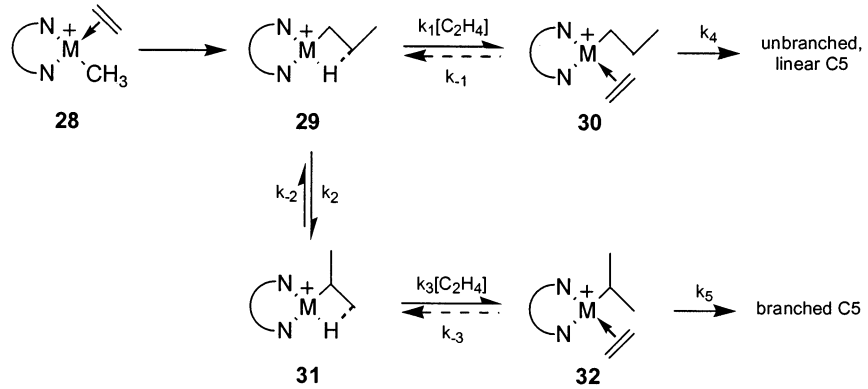

Movement from C1 to C3 (**24** to **27**) requires breaking the H2 agostic interaction, rotation about M−C1, formation of an agostic interaction with H3 (**24** to **26**), followed by β-elimination/readdition (**26** to **27**). In the case of palladium, β-elimination is the lower energy barrier ($\Delta G^{\ddagger} \approx 7$ kcal/mol). The barrier to rotation about Pd−C1 is estimated as ca. 9−10 kcal/mol and is thus the barrier that controls the rate of metal migration along the chain. In the case of nickel, the Ni−C1 rotational barrier is comparable to the Pd barrier (ca. 9.0−9.5 kcal/mol), but the β-elimination barrier of 14.0 kcal/mol is higher than either Pd barrier and controls the rate of chain migration of Ni. This substantial difference in barriers of ca. 4−5 kcal/mol, resulting in a much slower migration of Ni along the chain, clearly has an impact on the extent of branching in the polyethylenes and is discussed in more detail below.

When chain walking occurs from the alkyl ethylene complexes, a question arises as to whether these isomerization reactions occur through a five-coordinate intermediate or via reversible ethylene loss to yield the highly dynamic metal alkyl agostic complexes. For palladium complexes, the mechanism was clearly shown to be ethylene loss followed by isomerization of the agostic Pd alkyl species.[33,34] Since nickel is more prone to form five-coordinate species, confirmation of the ligand loss mechanism was sought. Indeed, as with the Pd systems, this mechanism was verified in the case of (diimine)NiR(L)$^+$ (L = CH_3CN, Me_2S) by demonstrating that chain isomerization is retarded by added L, an observation inconsistent with a nondissociative, five-coordinate intermediate. Since ethylene and CH_3CN have similar binding affinities, it can be reasonably assumed that a dissociative mechanism applies in the case of L = C_2H_4.

Formation of Branched Polyethylenes. At similar reaction temperatures and ethylene pressures, palladium diimine catalysts yield much more highly branched polymers than their nickel analogues.[12,13] In contrast to Pd catalysts, the branching density in Ni systems is quite sensitive to temperature and ethylene pressure. The data reported here coupled with earlier mechanistic studies of the Pd systems provide a clear explanation for the differences in behavior of the Ni and Pd catalysts. The general mechanism for formation of branched polymers was shown earlier in Scheme 1, but to simplify discussion of this scheme, a simple model system is shown below in Scheme 15, which involves sequential insertion of two ethylene units into a M−CH_3 bond to form either a linear or branched C5 chain.

In the case of Pd, ethylene complexation is reversible and complexes **30** and **32** are in rapid equilibrium prior to migratory insertion.[33] The fraction of branched product produced is controlled by the equilibrium ratio of **32**/**30** times the ratio of rate constants k_5/k_4 (Curtin−Hammett kinetics). Translating this result to Scheme 1 implies that Pd can migrate over a large number of carbons prior to insertion, and since migration through tertiary carbon centers is facile,[34] highly branched polymers containing branches-on-branches (hyperbranched structures) are formed. At very high ethylene pressures the equilibrium ratio [(diimine)Pd(R)(C_2H_4)$^+$]/[(diimine)PdR$^+$ + C_2H_4]can be shifted so far toward the alkyl ethylene complex that the number of carbons, on average, over which Pd can migrate prior to insertion can be significantly reduced. As shown by Guan et al.,[17] this results in a change of polymer architecture from a hyperbranched structure to a more linear structure with fewer branches-on-branches even though the total number of branches per 1000 carbons remains essentially constant.

The Ni systems follow a similar mechanistic scheme, but, as noted, branching is much reduced and branching density is sensitive to temperature and ethylene pressure. At the low temperatures used here for mechanistic work, virtually no branching is observed. Referring to Scheme 15, no branched C5 product is formed as experimentally demonstrated above. This arises for two reasons. First, the β-elimination barrier, **29** to **31**, is much higher than in the case of Pd, and trapping of **29** by ethylene is thus fast relative to formation of **31**. Second, once formed, the low insertion barrier of **30** ensures that loss of ethylene to re-form **29** (and potentially equilibrate **30** and **32**) does not occur ($k_{-1} < k_4$). These arguments are further supported by the observation that isopropyl ethylene complex **32** (formed by trapping of **31**) does not form the isomeric and more stable *n*-propyl ethylene complex **30** prior to insertion.

As the temperature is increased, the first-order rate of β-elimination will increase faster than the second-order ethylene trapping rate and thus favor increased branching (in Scheme 15, $k_2/k_1[C_2H_4]$ increases with temperature). In addition, the ratio of (diimine)NiR$^+$/(diimine)Ni(R)(C_2H_4)$^+$ will increase with increasing temperature, favoring increased chain walking relative to insertion. Indeed, in Ni systems the rate of chain growth at higher temperatures shows some dependence on [C_2H_4] and suggests that the catalyst resting state is a mix of (diimine)Ni(R)(C_2H_4)$^+$ and (diimine)Ni(R)$^+$. Furthermore, we have shown that for the bulkier olefin propylene the resting state is the

(47) Density functional calculations suggest a concerted β-H elimination/olefin rotation/reinsertion process rather than a stepwise mechanism: Deng, L.; Margl, P.; Ziegler, T. *J. Am. Chem. Soc.* **1997**, *119*, 1094−1100.

agostic Ni alkyl complex, even at very low temperatures. Decreasing ethylene pressure increases the extent of branching for obvious reasons. The rate of chain walking relative to the rate of trapping ($k_1[C_2H_4]$ vs k_2) and the ratio of (diimine)Ni-$(R)^+$ to (diimine)Ni$(R)(C_2H_4)^+$ is increased as ethylene pressure is decreased.

Increased bulk of the diimine ligand (e.g., the diisopropyl-(aryl)- vs the dimethyl(aryl)-substituted ligand) favors increased branching. This is likely due to a decreased trapping rate of the more sterically hindered alkyl complex relative to the rate of chain walking. Theoretical calculations support decreased ethylene trapping rates of complexes containing sterically bulky ligands.[48]

Experimental Section

General Methods. All manipulations of air- and/or water-sensitive compounds were performed using standard high-vacuum or Schlenk techniques. Argon was purified by passage through columns of BASF R3-11 catalyst (Chemalog) and 4 Å molecular sieves. Solid organometallic compounds were transferred in argon-filled Vacuum Atmospheres or MBraun dryboxes. ^{1}H and ^{13}C NMR spectra were recorded on Bruker Avance 300, 400, or 500 MHz spectrometers. Chemical shifts are reported relative to residual $CHDCl_2$ (δ 5.32 for ^{1}H), $CHCl_2F$ (^{1}H, doublet centered at δ 7.47, J = 50 Hz), $CHClF_2$ (δ = 7.16 for ^{1}H), CD_2Cl_2 (δ 53.80 for ^{13}C), or $CDCl_3$ in $CDCl_2F$ solutions (δ 77.00 for ^{13}C).

Materials. Diethyl ether, pentane, and methylene chloride were purified using procedures recently reported by Pangborn et al.[49] Polymer-grade ethylene was purchased from National Specialty Gases and used without further purification. The α-diimine ligands (ArN═C(An)−C(An)═NAr, An,An = acenaphthyl = 1,8-naphthdiyl) and corresponding (α-diimine)nickel(II) bromide complexes were prepared according to modified literature procedures.[13,50−52] Nickel methyl ether adduct **2** was prepared as described previously.[32] (DME)$NiBr_2$,[53] $[H(OEt_2)_2]^+[BAr'_4]^-$ ($BAr'_4{}^- = B(3,5\text{-}C_6H_3(CF_3)_2)_4^-$),[54] and $[H(O^iPr_2)_2]^+$-$[BAr'_4]^-$[55] were prepared according to literature procedures. Diisopropyl ether was distilled from potassium/benzophenone ketyl under argon. Dichlorofluoromethane-*d* was prepared according to the literature[56] and was purified by stirring over silica gel to remove silane byproducts,[57] dried over CaH_2, vacuum transferred, and degassed by repeated freeze−pump−thaw cycles. Dichloromethane-d_2 was dried over P_2O_5, vacuum transferred, degassed by repeated freeze−pump−thaw cycles, and stored over activated 4 Å molecular sieves. Acenaphthenequinone, 2,6-dimethylaniline, 2,6-diisopropylaniline, EtMgBr, and PrMgBr were purchased from Aldrich Chemical Co. and used as received. Anhydrous acetonitrile and dimethyl sulfide were purchased from Aldrich Chemical Co. and used as received. $NaBAr'_4$ was purchased from Boulder Scientific.

Synthesis of Nickel Dialkyl Complexes. (ArN═C(An)−C(An)═NAr)Ni$(CH_2CH_2CH_3)_2$ (Ar = 2,6-C_6H_3(Me)$_2$), 7. A Schlenk flask was equipped with a magnetic stir bar and flame-dried under vacuum. The flask was charged with (diimine)$NiBr_2$ **5** (1.00 g, 1.65 mmol) in the drybox and sealed with a rubber septum that had been previously dried overnight at 100 °C. Dry diethyl ether (30 mL) was added to the flask via syringe. The resulting red-brown slurry was stirred at room temperature for 15 min, then cooled to −78 °C under argon. After 15 min, PrMgBr (1.65 mL of a 2.0 M Et_2O solution, 3.30 mmol) was slowly added dropwise. The reaction slurry immediately changed to a very dark blue color. After 3 h at −78 °C, the stirring was ceased and the reaction mixture allowed to settle for 10 min. A jacketed filter frit was charged with Florisil (2 cm wide by 1 cm deep column), attached to a Schlenk flask, and the entire assembly was flame-dried under vacuum. Upon cooling, the filter frit assembly was back-filled with argon, and the Florisil column and Schlenk flask were cooled to −78 °C. Dry diethyl ether (10 mL) was added to the top of the Florisil column, the receiver flask was vented to an argon-purged oil bubbler, and the reaction mixture was quickly transferred to the filter frit using a 12-gauge cannula. It is critical to transfer the solution as fast as possible; reductive elimination of hexane occurs if the solution warms appreciably in the cannula. The entire solution was forced through the Florisil as fast as possible under argon head pressure. The filtered solution was filtered a second time through a filter cannula into another flame-dried Schlenk flask cooled to −78 °C, and the solvent was removed under vacuum at ca. −40 °C. The flask was quickly taken into the drybox, and the dark solid purple product was recovered (610 mg, 69%). This manipulation of the product was performed at room temperature, but as quickly as practical. The product is stable when stored below −15 °C in the drybox, but decomposes within an hour at room temperature. CD_2Cl_2 solutions of the product decompose in minutes at room temperature, turning from the characteristic blue color of the desired nickel dipropyl complex to a purple color. The structure of the complex(es) formed at this point are unknown. Exposure of the purple solution to air results in the immediate formation of a black heterogeneous solution. In addition, the isolated nickel dipropyl complex is extremely air-sensitive and decomposes immediately upon exposure to oxygen, forming a black solid. The product was characterized by low-temperature ^{1}H NMR, ^{13}C NMR, ^{1}H−^{1}H COSY, and ^{13}C DEPT NMR experiments. ^{1}H NMR (CD_2Cl_2, −80 °C, 300 MHz): δ 8.31 (d, J = 8.3 Hz, 2H, An H_p), 7.47−7.37 (m, 6H, Ar*H*), 7.06 (apparent t (overlapping doublets), 2H, An H_m), 6.65 (d, J = 7.1 Hz, 2H, An H_o), 2.30 (br t, 4H, NiC*H*$_2$), 2.22 (s, 12H, ArC*H*$_3$), 0.53 (br s, 10H, coincidental overlap of $NiCH_2CH_2CH_3$ and $NiCH_2CH_2CH_3$). ^{13}C NMR (CD_2Cl_2, −80 °C, 100 MHz): δ 162.7 (N═*C*−*C*═N), 149.2, 136.7, 133.4, 133.2, 130.1, 127.84, 127.78, 125.9, 125.4, 118.7, 23.3 (Ni*C*H$_2$ or $NiCH_2CH_2$), 18.06 (Ar*C*H$_3$), 18.01 ($NiCH_2CH_2CH_3$), 15.9 (Ni*C*H$_2$ or $NiCH_2CH_2$).

(ArN═C(An)−C(An)═NAr)Ni$(CH_2CH_2CH_3)_2$ (Ar = 2,6-C_6H_3-(^{i}Pr)$_2$), 8. This compound was prepared using the same procedure described above for **7**. (Diimine)$NiBr_2$ **6** (0.750 g, 1.04 mmol) and PrMgBr (1.15 mL of a 2.0 M Et_2O solution, 2.30 mmol) were used as starting materials. Using the workup described above, 291 mg (43%) of the purple solid product was recovered. Et_2O and CH_2Cl_2 solutions of the product are dark blue in color. Solutions of the product decompose at temperatures above −20 °C, producing hexane and unidentified products; the solution is purple and homogeneous. Exposure of the purple solution to air results in immediate decomposition to a black heterogeneous solution. The product was characterized by low-temperature ^{1}H, ^{13}C, ^{1}H−^{1}H COSY, and ^{13}C DEPT NMR experiments. ^{1}H NMR (CD_2Cl_2, −60 °C, 400 MHz): δ 8.27 (d, J = 8.0, 2H, An H_p), 7.60 (br m, 2H, Ar H_p), 7.50 (br d, 4H, Ar H_m), 7.03 (apparent t (overlapping doublets), 2H, An H_m), 6.49 (d, J = 7.2, 2H, An H_o), 3.34 (br m, 4H, ArC*H*MeMe′), 2.86 (q, J = 7.2, 4H, $NiCH_2CH_2CH_3$), 1.36 (d, J = 6.4, 12H, ArCH*Me*Me′), 0.71 (d, J = 6.4, 12H, ArCHMe*Me*′), 0.57 (t, J = 6.4, 6H, $NiCH_2CH_2CH_3$), 0.27 (br m, 4H, $NiCH_2CH_2CH_3$). ^{13}C NMR (CD_2Cl_2, −60 °C, 100 MHz): δ 162.4 (N═*C*−*C*═N), 146.9, 138.6, 136.2, 134.1, 133.6, 130.1, 126.3, 125.7, 123.5,

(48) Woo, T. K.; Blöchl, P. E.; Ziegler, T. *J. Phys. Chem. A* **2000**, *104*, 121−129.
(49) Pangborn, A. B.; Giardello, M. A.; Grubbs, R. H.; Rosen, R. K.; Timmers, F. J. *Organometallics* **1996**, *15*, 1518−1520.
(50) van Asselt, R.; Elsevier, C. J.; Smeets, W. J. J.; Spek, A. L.; Benedix, R. *Recl. Trav. Chim. Pays-Bas* **1994**, *113*, 88−98.
(51) Tom Dieck, H.; Svoboda, M.; Grieser, T. *Z. Naturforsch.* **1981**, *36b*, 823−832.
(52) Svoboda, M.; Tom Dieck, H. *J. Organomet. Chem.* **1980**, *191*, 321−328.
(53) Ward, L. G. L. *Inorg. Synth.* **1971**, *13*, 154−164.
(54) Brookhart, M.; Grant, B.; Volpe, A. F. *Organometallics* **1992**, *11*, 3920−3922.
(55) White, P. A.; Calabrese, J.; Theopold, K. H. *Organometallics* **1996**, *15*, 5473−5475.
(56) Siegel, J. S.; Anet, F. A. *J. Org. Chem.* **1988**, *53*, 2629−2630.
(57) A small amount of Me_2SiF_2 was occasionally observed as a byproduct of the fluorination reaction. Formation of this product can be suppressed through minimal use of silicone grease on glass joints used in the preparation of $CDCl_2F$.

119.7, 28.1 (Ar*C*HMeMe′), 24.0 (Ni*C*H_2CH$_2$CH$_3$ or NiCH$_2$*C*H_2CH$_3$), 23.3 (ArCH*Me*Me′), 23.0 (ArCHMe*Me*′), 17.7 (NiCH$_2$CH$_2$*C*H$_3$), 16.7 (Ni*C*H_2CH$_2$CH$_3$ or NiCH$_2$*C*H_2CH$_3$).

(ArN═C(An)−C(An)═NAr)Ni(CH$_2$CH$_3$)$_2$ (Ar = 2,6-C$_6$H$_3$(Me)$_2$), 9. This compound was prepared using the same procedure described above for **7**. (Diimine)NiBr$_2$ **5** (1.00 g, 1.65 mmol) and EtMgBr (1.65 mL of a 2.0 M Et$_2$O solution, 3.30 mmol) were used as starting materials. Using the workup described above, 610 mg (69%) of the purple solid product was recovered. Et$_2$O and CH$_2$Cl$_2$ solutions of the product are dark blue in color. Solutions of the product decompose at temperatures above −20 °C, producing butane and unidentified products; the solution is purple and homogeneous. Exposure of the purple solution to air results in immediate decomposition to a black heterogeneous solution. The product was characterized by low-temperature ^{1}H, ^{13}C, ^{1}H−^{1}H COSY, and ^{13}C DEPT NMR experiments. ^{1}H NMR (CD$_2$Cl$_2$, −80 °C, 400 MHz): δ 8.28 (d, J = 8.0 Hz, 2H, An H$_p$), 7.46−7.40 (m, 6H, Ar*H*), 7.07 (apparent t (overlapping doublets), 2H, An H$_m$), 6.59 (d, J = 7.0 Hz, 2H, An H$_o$), 2.23 (s, 12H, ArC*H*$_3$), 2.12 (q, J = 7.6 Hz, 4H, NiC*H*$_2$), 0.22 (t, J = 7.6 Hz, 6 H, NiCH$_2$C*H*$_3$). ^{13}C NMR (CD$_2$Cl$_2$, −80 °C, 100 MHz): δ 163.5 (N═*C*−*C*═N), 148.8, 136.9, 133.0, 132.9, 130.0, 127.9 (2 overlapping signals), 126.1, 125.5, 118.9, 18.0 (Ar*C*H$_3$), 14.1 (NiCH$_2$*C*H$_3$), 6.4 (Ni*C*H$_2$).

(ArN═C(An)−C(An)═NAr)Ni(CH$_2$CH$_3$)$_2$ (Ar = 2,6-C$_6$H$_3$(^{i}Pr)$_2$), 10. This compound was prepared using the same procedure described above for **7**. (Diimine)NiBr$_2$ **6** (0.750 g, 1.04 mmol) and EtMgBr (1.15 mL of a 2.0 M Et$_2$O solution, 2.30 mmol) were used as starting materials. Using the workup described above, 439 mg (68%) of the purple solid product was recovered. Et$_2$O and CH$_2$Cl$_2$ solutions of the product are dark blue in color. Solutions of the product decompose at temperatures above −20 °C, producing butane and unidentified products; the solution is purple and homogeneous. Exposure of the purple solution to air results in immediate decomposition to a black heterogeneous solution. The product was characterized by low-temperature ^{1}H, ^{13}C, ^{1}H−^{1}H COSY, and ^{13}C DEPT NMR experiments. ^{1}H NMR (CD$_2$Cl$_2$, −60 °C, 400 MHz): δ 8.27 (d, J = 8.0, 2H, An H_p), 7.61 (apparent t (overlapping doublets), 2H, Ar H_p), 7.49 (d, J = 10.4, 4H, Ar H_m), 7.04 (apparent t (overlapping doublets), 2H, An H_m), 6.51 (d, J = 6.8, 2H, An H_o), 3.28 (septet, J = 8.8, 4H, ArC*H*MeMe′), 2.67 (q, J = 7.2, 4H, NiC*H*$_2$CH$_3$), 1.34 (d, J = 5.6, 12H, ArCH*Me*Me′), 0.73 (d, J = 6.0, 12H, ArCHMe*Me*′), 0.06 (t, 6H, NiCH$_2$C*H*$_3$). ^{13}C NMR (CD$_2$Cl$_2$, −60 °C, 100 MHz): δ 163.2 (N═*C*−*C*═N), 147.0, 138.6, 136.4, 133.9, 133.6, 130.1, 126.4, 125.9, 123.6, 119.8, 28.4 (Ar*C*HMeMe′), 23.5 (ArCH*Me*Me′), 23.1 (ArCHMe*Me*′), 15.3 (NiC-H$_2$*C*H$_3$), 6.3 (Ni*C*H$_2$CH$_3$).

Synthesis of β-Agostic Isopropyl Complexes. [(ArN═C(An)−C(An)═NAr)Ni(CH(CH$_2$-μ-H)(CH$_3$))]$^+$[BAr$_4$′]$^-$ (Ar = 2,6-C$_6$H$_3$Me$_2$), *i*-11. Two Schlenk tubes were equipped with stir bars, fitted with rubber septa, flame-dried, and taken into a drybox. The nickel dipropyl complex **7** (101 mg, 0.19 mmol) was added to one tube, and [H(OEt$_2$)$_2$]$^+$[BAr′$_4$]$^-$ (202 mg, 0.20 mmol) was added to the other. The tubes were sealed, placed on a Schlenk line, and cooled to −78 °C. After 5 min, 10 mL of dry CH$_2$Cl$_2$ was slowly added to each tube at −78 °C. The solutions were stirred to fully dissolve the solids (15 min), and the oxonium acid solution was then cooled to −100 °C (pentane/liquid N$_2$ slurry). The solution of the nickel dipropyl complex **7** was quickly added to the stirred solution of the oxonium acid via cannula. The reaction was initially the deep blue color of the nickel dipropyl complex. The reaction mixture was allowed to warm to −78 °C over 30 min and slowly turned a darker midnight-blue color. The reaction was stirred at −78 °C for 2 h, during which time no apparent color change was observed. The reaction was allowed to warm slowly to −30 °C, and all solvent was removed in vacuo at −30 °C. The maroon-black solid was dried in vacuo at −20 °C for 2 h, recovered in the drybox (221 mg, 86%), and stored at −35 °C. The product was characterized by low-temperature ^{1}H NMR and ^{1}H−^{1}H COSY NMR. At −120 °C, the product appears to be a 20:1 mixture of the β-agostic isopropyl species ***i*-11**/β-agostic *n*-propyl species ***n*-11**. ^{1}H NMR (CDCl$_2$F, −130 °C, 400 MHz): δ 8.12 (apparent t (overlapping doublets), 2H, An H_p and H_p′), 7.85 (s, 8H, BAr$_4$′), 7.55−7.27 (m, 8H, Ar*H*), 7.53 (s, 4H, BAr$_4$′), 6.89 (d, J = 7.3 Hz, 1H, An H$_o$), 6.74 (d, J = 7.3 Hz, 1H, An H$_o$′), 2.43, 2.41, 2.37, 2.25 (all s, 3H each, ArC*H*$_3$, ArC*H*$_3$′, ArC*H*$_3$″, ArC*H*$_3$‴), 2.00 (m, 1H, NiC*H*), 0.26 (br m, 1H, C*H*H′(μ-H)), 0.11 (br m, 1H, CH*H*′(μ-H)), −0.09 (br s, 3H, C*H*$_3$), −12.49 (t, $^2J_{HH}$ = 19 Hz, 1H, μ-*H*). *n*-propyl β-agostic species ***n*-11**: δ −13.0 (d, $^2J_{HH}$ = 19 Hz).

[(ArN═C(An)−C(An)═NAr)Ni(CH(CH$_2$-μ-H)(CH$_3$))]$^+$[BAr$_4$′]$^-$ (Ar = 2,6-C$_6$H$_3$^{i}Pr$_2$), 12. A flame-dried Schlenk tube was charged with the nickel dipropyl complex **8** (100 mg, 0.155 mmol) and [H(OEt$_2$)$_2$]$^+$[BAr′$_4$]$^-$ (185 mg, 0.183 mmol) in the drybox. The tube was sealed and cooled to −80 °C under Ar, and CH$_2$Cl$_2$ (20 mL) was added slowly on the sides of the tube. The dark blue-black, homogeneous reaction solution was stirred at −80 °C for 30 min, then allowed to warm slowly to −20 °C. All solvent was removed in vacuo at −20 °C, and the maroon solid was dried in vacuo at 0 °C for 2 h, recovered in the drybox (138 mg, 61%), and stored at −35 °C. The product was characterized by low-temperature ^{1}H NMR and ^{1}H−^{1}H COSY NMR. ^{1}H NMR (CDCl$_2$F, −120 °C, 500 MHz): δ 8.08 (apparent t (overlapping doublets), 2H, An H_p and H_p′), 7.80 (s, 8H, BAr$_4$′), 7.55−7.42 (m, 8H, Ar*H*), 7.53 (s, 4H, BAr$_4$′), 6.83 (d, J = 5.6 Hz, 1H, An H$_o$), 6.78 (d, J = 6.0 Hz, 1H, An H$_o$′), 3.47, 3.38, 3.18, 3.09 (all br septets, 1H each, ArC*H*(CH$_3$)$_2$, ArC*H*′(CH$_3$)$_2$, ArC*H*″(CH$_3$)$_2$, ArC*H*‴(CH$_3$)$_2$), 2.16 (septet, J = 5.2 Hz, 1H, NiC*H*), 1.56, 1.50, 1.44, 1.40, 1.14, 1.10, 1.04, 0.90 (all d, 3H each, ArCH(C*H*$_3$)$_2$), 0.67 (br m, 2H, C*H*H′(μ-H) and CH*H*′(μ-H)), −0.22 (br d, 3H, Ni(CHC*H*$_3$)), −12.49 (t, $^2J_{HH}$ = 18 Hz, 1H, μ-*H*).

Rates of Alkyl Isomerization and Migratory Insertion. Rates for alkyl isomerization of Ni(β-agostic alkyl) cations were measured by ^{1}H NMR line broadening techniques using the slow exchange approximation at various temperatures. NMR probe temperatures were calibrated using an Omega type T thermocouple immersed in anhydrous methanol in a 5 mm NMR tube. Activation parameters ($\Delta G^{\ddagger}$) were determined using the Eyring equation assuming an estimate of 10% error in k and ±0.1 °C in temperature. Rates for alkyl isomerization of Ni(^{i}Pr)L complexes were determined by monitoring the loss of the NiCH(C*H*$_3$)$_2$ resonances in the ^{1}H NMR spectra over time, as well as the appearance of the NiCH$_2$CH$_2$C*H*$_3$ resonance, using the BAr′$_4$ *p*-H signal as an internal reference. The natural logarithm of the number of equivalents of the NiCH(CH$_3$)$_2$ complex was plotted versus time (first-order treatment) to obtain kinetic plots (see Supporting Information). Rates for ethylene insertion were determined by monitoring the loss of the NiCH(C*H*$_3$)$_2$, NiCH$_2$CH$_2$C*H*$_3$, or NiCH$_2$C*H*$_3$ resonance as appropriate, using the BAr′$_4$ *p*-H signal as an internal reference. The natural logarithm of the starting alkyl ethylene complex resonance was plotted versus time (first-order treatment) to obtain kinetic plots (see Supporting Information).

Synthesis of Cationic Nickel Alkyl(L) Complexes (L = NCCH$_3$, S(CH$_3$)$_2$). [(ArN═C(An)−C(An)═NAr)NiCH(CH$_3$)$_2$)(NCCH$_3$)]$^+$[BAr$_4$′]$^-$ (Ar = 2,6-C$_6$H$_3$Me$_2$), *i*-16. β-Agostic complex ***i*-11** (13.9 mg, 0.0103 mmol) was quickly added to an NMR tube in the drybox. The tube was sealed with a septum, wrapped with Parafilm, and cooled to −80 °C. CD$_2$Cl$_2$ (0.6 mL) was added via gastight syringe, followed by a solution of NCCH$_3$ in CD$_2$Cl$_2$ (0.11 mL of a 0.187 M solution, 2 equiv of NCCH$_3$). The tube was shaken briefly to dissolve the solids, resulting in an immediate color change of the solution from the maroon of the free agostic cation to deep blue. The structure of ***i*-16** was confirmed by ^{1}H and ^{1}H−^{1}H COSY experiments. ^{1}H NMR (CD$_2$Cl$_2$, −60 °C, 400 MHz): δ 8.13 (apparent t (overlapping doublets), 2H, An H_p and H_p′), 7.70 (s, 8H, BAr$_4$′), 7.53 (s, 4H, BAr$_4$′), 7.48−7.28 (m, 8H, Ar*H*), 6.92 (d, J = 7.2 Hz, 1H, An H$_o$), 6.38 (d, J = 6.8 Hz, 1H, An H$_o$′), 2.39 (s, 6H, ArC*H*$_3$), 2.33 (s, 6H, ArC*H*$_3$′), 1.80 (br s, 6H, NCC*H*$_3$), 1.45 (m, 1H, Ni−C*H*), 0.27 (d, J = 6.0 Hz, 6H, CH-(C*H*$_3$)$_2$).

[(ArN=C(An)−C(An)=NAr)Ni(CH$_2$CH$_2$CH$_3$)(NCCH$_3$)]$^+$-[BAr$_4$′]$^-$ (Ar = 2,6-C$_6$H$_3$Me$_2$), *n*-16. This complex is observed in situ upon isomerization of ***i*-16** at temperatures above −10 °C. An equilibrium between the two complexes is slowly established, with a final ratio of 1:3 ***i*-16**/***n*-16** (−10 °C). The structure of ***n*-16** was confirmed by ^{1}H and ^{1}H−^{1}H COSY experiments. ^{1}H NMR (CD$_2$Cl$_2$, −60 °C, 400 MHz): δ 8.09 (apparent t (overlapping doublets), 2H, An H$_p$ and H$_p$′), 7.71 (s, 8H, BAr$_4$′), 7.51 (s, 4H, BAr$_4$′), 7.48−7.25 (m, 8H, Ar*H*), 6.91 (d, J = 7.2 Hz, 1H, An H$_o$), 6.31 (d, J = 7.2 Hz, 1H, An H$_o$′), 2.34 (s, 6H, ArC*H*$_3$), 2.26 (s, 6H, ArC*H*$_3$′), 1.91 (br s, 6H, NCC*H*$_3$), 1.00 (t, 2H, Ni−C*H*$_2$), 0.69 (br t, 3H, NiCH$_2$CH$_2$C*H*$_3$), 0.62 (m, 2H, NiCH$_2$C*H*$_2$CH$_3$).

[(ArN=C(An)−C(An)=NAr)NiCH(CH$_3$)$_2$)(S(CH$_3$)$_2$)]$^+$[BAr$_4$′]$^-$ (Ar = 2,6-C$_6$H$_3$Me$_2$), *i*-17. β-Agostic complex ***i*-11** (10.4 mg, 0.0077 mmol) was quickly added to an NMR tube in the drybox. The tube was sealed with a septum, wrapped with Parafilm, and cooled to −80 °C. CD$_2$Cl$_2$ (0.65 mL) was added via gastight syringe, followed by a solution of SMe$_2$ in CD$_2$Cl$_2$ (0.05 mL of a 0.154 M solution, 1 equiv of SMe$_2$). The tube was shaken briefly to dissolve the solids, resulting in an immediate color change of the solution from the maroon of the free agostic cation to emerald green. The structure of ***i*-17** was confirmed by ^{1}H and ^{1}H−^{1}H COSY experiments. ^{1}H NMR (CD$_2$Cl$_2$, −60 °C, 400 MHz): δ 8.10 (apparent t (overlapping doublets), 2H, An H$_p$ and H$_p$′), 7.71 (s, 8H, BAr$_4$′), 7.51 (s, 4H, BAr$_4$′), 7.46−7.27 (m, 8H, Ar*H*), 6.62 (d, J = 7.2 Hz, 1H, An H$_o$), 6.36 (d, J = 7.2 Hz, 1H, An H$_o$′), 2.42 (s, 6H, ArC*H*$_3$), 2.33 (s, 6H, ArC*H*$_3$′), 1.86 (br s, 6H, S(C*H*$_3$)$_2$), 1.52 (m, 1H, Ni−C*H*), −0.07 (d, J = 6.0 Hz, 6H, CH(C*H*$_3$)$_2$).

[(ArN=C(An)−C(An)=NAr)Ni(CH$_2$CH$_2$CH$_3$)(S(CH$_3$)$_2$)]$^+$-[BAr$_4$′]$^-$ (Ar = 2,6-C$_6$H$_3$Me$_2$), *n*-17. This complex exists in a mixture with the isopropyl complex ***i*-17** upon SMe$_2$ trapping of ***i*-11** below −45 °C; at higher temperatures, the isopropyl species ***i*-17** isomerizes completely to yield ***n*-17**, confirmed by ^{1}H and ^{1}H−^{1}H COSY experiments. ^{1}H NMR (CD$_2$Cl$_2$, −20 °C, 400 MHz): δ 8.14 (d, J = 8.0 Hz, 1H, An H$_p$), 8.11 (d, J = 8.4 Hz, 1H, H$_p$′), 7.70 (s, 8H, BAr$_4$′), 7.53 (s, 4H, BAr$_4$′), 7.50−7.27 (m, 8H, Ar*H*), 6.65 (d, J = 7.2 Hz, 1H, An H$_o$), 6.51 (d, J = 7.2 Hz, 1H, An H$_o$′), 2.35 (s, 6H, ArC*H*$_3$), 2.33 (s, 6H, ArC*H*$_3$′), 1.93 (br s, 6H, S(C*H*$_3$)$_2$), 1.01 (m, 2H, Ni−CH$_2$C*H*$_2$-CH$_3$), 0.61 (br t, 3H, NiC*H*$_2$CH$_2$CH$_3$), 0.47 (t, J = 7.2 Hz, 2H, NiCH$_2$-CH$_2$C*H*$_3$).

Synthesis of β-Agostic Ethyl Complexes. [(ArN=C(An)−C(An)=NAr)Ni(CH$_2$(CH$_2$-μ-H))]$^+$[BAr$_4$′]$^-$ (Ar = 2,6-C$_6$H$_3$Me$_2$), 18. Nickel diethyl complex **9** (5.3 mg, 10.5 μmol) and [H(O^{i}Pr$_2$)$_2$][BAr′$_4$] (11.2 mg, 10.5 μmol) were placed in a screw-cap NMR tube in the drybox. A solution of CDCl$_2$F (∼700 μL) was added to the tube via cannula at −80 °C. The tube was briefly agitated to dissolve the sample, and the resulting solution was dark maroon and homogeneous. The sample was then transferred to a NMR probe precooled to −130 °C. The structure of **18** was confirmed by ^{1}H and ^{1}H−^{1}H COSY NMR experiments. ^{1}H NMR (CDCl$_2$F, −120 °C, 400 MHz): δ 8.08 (apparent t (overlapping doublets), 2H, An H$_p$ and H$_p$′), 7.82 (s, 8H, BAr$_4$′), 7.55 (s, 4H, BAr$_4$′), 7.42−7.35 (m, 8H, Ar*H*), 6.90 (d, J = 6.8 Hz, 1H, An H$_o$), 6.71 (d, J = 6.8 Hz, 1H, An H$_{o'}$), 2.41 (s, 6 H, ArC*H*$_3$), 2.37 (s, 6 H, ArC*H*′$_3$), 1.22 (br m, 2 H, NiC*H*$_2$CH$_2$(μ-H)), 0.41 (br m, 2H, NiCH$_2$C*H*$_2$(μ-H)), −13.7 (br t, 1H, NiCH$_2$CH$_2$(μ-*H*)). Ethane and diisopropyl ether are also present in the sample.

[(ArN=C(An)−C(An)=NAr)Ni(CH$_2$(CH$_2$-μ-H))]$^+$[BAr$_4$′]$^-$ (Ar = 2,6-C$_6$H$_3$^{i}Pr$_2$), 19. Nickel diethyl complex **10** (7.5 mg, 12.1 μmol) and [H(O^{i}Pr$_2$)$_2$][BAr′$_4$] (14.6 mg, 13.6 μmol) were placed in a screw-cap NMR tube in the drybox. A solution of CDCl$_2$F (∼700 μL) was added to the tube via cannula at −80 °C. The tube was briefly agitated to dissolve the sample, and the resulting solution was dark maroon and homogeneous. The sample was then transferred to a NMR probe precooled to −130 °C. The structure of **19** was confirmed by ^{1}H and ^{1}H−^{1}H COSY NMR experiments. ^{1}H NMR (CDCl$_2$F, −130 °C, 500 MHz): δ 8.05 (apparent t (overlapping doublets), 2H, An H$_p$ and H$_p$′), 7.70 (s, 8H, BAr$_4$′), 7.52−7.42 (m, 8H, Ar*H*), 7.51 (s, 4H, BAr$_4$′), 6.84 (d, J = 7.5 Hz, 1H, An H$_o$), 6.70 (d, J = 8.0 Hz, 1H, An H$_{o'}$), 1.45, 1.39, 1.25, 0.99 (all br d, 6H each, Ar(CH(C*H*$_3$))), 0.35 (br m, 2H, NiCH$_2$C*H*$_2$(μ-H)), −13.8 (t, J = 19.0 Hz, 1H, NiCH$_2$CH$_2$(μ-*H*)). The NiC*H*$_2$CH$_2$(μ-H) resonance is obscured by ligand Ar(CH(C*H*$_3$)$_2$) signals, but was identified in the ^{1}H−^{1}H COSY spectrum (δ 1.42) via coupling to both the agostic and nonagostic protons of the terminal methyl group. Ethane, diisopropyl ether, and a small amount of residual [H(O^{i}Pr$_2$)$_2$]$^+$-[BAr′$_4$]$^-$ are also present in the sample.

Synthesis of Alkyl Olefin Complexes. [(ArN=C(An)−C(An)=NAr)NiCH(CH$_3$)$_2$)(C$_2$H$_4$)]$^+$[BAr$_4$′]$^-$ (Ar = 2,6-C$_6$H$_3$Me$_2$), *i*-13. β-Agostic isopropyl complex ***i*-11** (∼13 mg, 10 μmol) was placed in an NMR tube in the drybox. The tube was quickly capped with a rubber septum, wrapped with Parafilm, and cooled to −130 °C. A solution of CDCl$_2$F/CDClF$_2$ (1:1, ∼700 μL) was added to the tube via cannula. Ethylene (0.5 mL, ca. 2 equiv) was added to the solution via gastight syringe at −130 °C. The tube was briefly agitated to dissolve the sample, and the resulting solution was red and homogeneous. The sample was then transferred to a NMR probe precooled to −130 °C. The structure of ***i*-13** was confirmed by ^{1}H and ^{1}H−^{1}H COSY NMR experiments. No agostic hydrogen resonances were observed at −130 °C. ^{1}H NMR (CDCl$_2$F/CDClF$_2$ (1:1), −130 °C, 500 MHz): δ 8.09 (apparent t (overlapping doublets), 2H, An H$_p$ and H$_p$′), 7.83 (s, 8H, BAr$_4$′), 7.49 (s, 4H, BAr$_4$′), 7.51−7.30 (m, 8H, Ar*H*), 6.70 (apparent t (overlapping doublets), 2H, An H$_o$ and H$_o$′), 3.96 (d, J = 14 Hz, 2H, bound C*H*H′=C*H*H′), 3.53 (d, J = 14 Hz, 2H, bound CH*H*′=CH*H*′), 2.28 (s, 6H, ArC*H*$_3$), 2.23 (s, 6H, ArC*H*$_3$′), 1.47 (m, 1H, Ni−C*H*), 0.40 (br s, 6H, CH(C*H*$_3$)$_2$).

[(ArN=C(An)−C(An)=NAr)Ni(CH$_2$CH$_2$CH$_3$)(C$_2$H$_4$)]$^+$[BAr$_4$′]$^-$ (Ar = 2,6-C$_6$H$_3$Me$_2$), *n*-13. Nickel dipropyl complex **8** (6.5 mg, 1.2 X 10^{-5} mol) and [H(OEt$_2$)$_2$]$^+$[BAr′$_4$]$^-$ (11.6 mg, 1.2 × 10^{-5} mol) were combined as solids in an NMR tube in the drybox. The tube was quickly sealed with a rubber septum, wrapped with Parafilm, and cooled to −130 °C. Ethylene (1.0 mL, ∼4 equiv) was added to the tube via gastight syringe. The tube was briefly immersed in liquid nitrogen, and a mixture of CDCl$_2$F/CDClF$_2$ (1:1) was added via cannula. Initially, a near-black solution was formed. The NMR tube was placed in the NMR probe, which had been precooled to −130 °C. The presence of the nickel *n*-propyl group was confirmed by low-temperature ^{1}H NMR and ^{1}H−^{1}H COSY NMR. No agostic hydrogen resonances were observed at −130 °C. ^{1}H NMR (CDCl$_2$F/CDClF$_2$ (1:1), −100 °C, 500 MHz): δ 8.11 (d, J = 8.3 Hz, 1H, An H$_p$), 8.07 (d, J = 8.3 Hz, 1H, An H$_p$′), 7.84 (s, 8H, BAr$_4$′), 7.56 (s, 4H, BAr$_4$′), 7.54−7.29 (m, 8H, Ar*H*), 6.78 (d, J = 7.3 Hz, 1H, An H$_o$), 6.71 (d, J = 7.3 Hz, 1H, An H$_o$′), 5.47 (very br, free C$_2$*H*$_4$), 4.17 (br d, 2H, bound C*H*H′=C*H*H′), 3.31 (br d, 2H, bound CH*H*′=CH*H*′), 2.38 (s, 6H, ArC*H*$_3$), 2.29 (s, 6H, Ar′C*H*$_3$), 1.22 (m, 2H, NiCH$_2$C*H*$_2$CH$_3$), 0.61 (t, J = 6.9 Hz, 3H, NiCH$_2$CH$_2$C*H*$_3$), 0.48 (t, J = 7.5 Hz, 2H, NiC*H*$_2$CH$_2$CH$_3$). Propane, diethyl ether, and a small amount of residual [H(OEt$_2$)$_2$]$^+$[BAr′$_4$]$^-$ are also present in the sample. The sample was observed to be a red homogeneous solution upon removal from the NMR probe.

[(ArN=C(An)−C(An)=NAr)Ni(CH$_2$CH$_3$)(C$_2$H$_4$)]$^+$[BAr$_4$′]$^-$ (Ar = 2,6-C$_6$H$_3$^{i}Pr$_2$), 22. Nickel diethyl complex **13** (6.0 mg, 9.7 μmol) and [H(O^{i}Pr$_2$)$_2$][BAr′$_4$] (14.3 mg, 13.4 μmol) were placed in a screw-cap NMR tube in the drybox. A solution of CDCl$_2$F (∼700 μL) was added to the tube via cannula at −80 °C. The tube was briefly agitated to dissolve the sample, and the resulting solution was dark maroon and homogeneous. Ethylene (2.4 mL, ca. 10 equiv) was added to the solution via gastight syringe at −130 °C. The sample was then transferred to a NMR probe precooled to −130 °C. The structure of **22** was confirmed by ^{1}H and ^{1}H−^{1}H COSY NMR experiments. No agostic hydrogen resonances were observed at −130 °C. ^{1}H NMR (CDCl$_2$F, −100 °C, 500 MHz): δ 8.02 (apparent t (overlapping doublets), 2H, An H$_p$ and H$_p$′), 7.80 (s, 8H, BAr$_4$′), 7.54 (s, 4H, BAr$_4$′), 7.50−7.42 (m, 8H, Ar*H*), 6.57 (d, J = 6.5 Hz, 1H, An H$_o$), 6.51 (d, J = 6.5 Hz, 1H, An H$_{o'}$), 5.42 (very br, free C$_2$*H*$_4$), 3.95 (br d, 2H, bound C*H*H′=C*H*H′), 3.69 (br d, 2H, bound CH*H*′=CH*H*′), 3.32 (br m, 2H, ArC*H*(CH$_3$)$_2$), 3.07

(br septet, 2H, ArC*H*′$(CH_3)_2$), 1.42 (br d, 6H, ArCH(C*H*$_3)_2$), 1.33 (br d, 6H, ArCH(C*H*′$_3)_2$), 0.93 (br, 12H, ArCH(C*H*″$_3)_2$ and ArCH(C*H*‴$_3)_2$), 0.85 (br m, 2H, NiC*H*$_2$CH$_3$), 0.65 (br t, 3H, NiCH$_2$C*H*$_3$). Ethane, diisopropyl ether, and a small amount of residual $[H(O^iPr_2)_2]^+[BAr'_4]^-$ are also present in the sample.

[(ArN═C(An)−C(An)═NAr)NiCH(CH$_3$)$_2$)(C$_2$H$_4$)]$^+$[BAr$_4$′]$^-$ (Ar = 2,6-C$_6$H$_3$^{i}Pr$_2$), 23. β-Agostic isopropyl complex **12** (9.0 mg, 6.1 μmol) was placed in an NMR tube in the drybox. The tube was quickly capped with a rubber septum, wrapped with Parafilm, and cooled to −130 °C. A solution of $CDCl_2F$ (∼700 μL) was added to the tube via cannula. Ethylene (1.5 mL, ca. 10 equiv) was added to the solution via gastight syringe at −130 °C. The tube was briefly agitated to dissolve the sample, and the resulting solution was red and homogeneous. The sample was then transferred to a NMR probe precooled to −130 °C. The structure of **23** was confirmed by ^{1}H and ^{1}H−^{1}H COSY NMR experiments. No agostic hydrogen resonances were observed at −130 °C. ^{1}H NMR ($CDCl_2F$, −100 °C, 500 MHz): δ 8.02 (apparent t (overlapping doublets), 2H, An H_p and H_p′), 7.78 (s, 8H, BAr$_4$′), 7.54 (s, 4H, BAr$_4$′), 7.49−7.42 (m, 8H, Ar*H*), 6.49 (br d, 1H, An H_o), 6.45 (br d, 1H, An H_o′), 5.43 (very br, free C_2H_4), 4.16 (d, J = 13.5 Hz, 2H, bound C*H*H′═C*H*H′), 3.60 (d, J = 14.5 Hz, 2H, bound CH*H*′═CH*H*′), 3.17 (br, 2H, ArC*H*$(CH_3)_2$), 2.80 (br, 2H, ArC*H*′$(CH_3)_2$), 1.38 (br d, 6H, ArCH(C*H*$_3)_2$), 1.29 (br d, 6H, ArCH(C*H*′$_3)_2$), 0.91 (br, 12H, ArCH-(C*H*″$_3)_2$ and ArCH(C*H*‴$_3)_2$), 1.82 (m, 1H, Ni−C*H*), 0.42 (br d, 6H, NiCH(C*H*$_3)_2$). Propane, diethyl ether, and a small amount of residual $[H(OEt_2)_2]^+[BAr'_4]^-$ are also present in the sample.

Acknowledgment. The authors wish to thank the NSF (Grant CHE-0107810) and DuPont for funding. S.A.S. acknowledges the United States Air Force Institute of Technology Civilian Institutions Program (AFIT/CI) for sponsorship.

Supporting Information Available: NMR spectra of representative (α-diimine)Ni(dialkyl) complexes, Ni(β-agostic alkyl) cations, Ni(alkyl)ethylene species, and Ni(alkyl)L complexes and graphs of kinetic data for ethylene insertion and alkyl isomerization. This material is available free of charge via the Internet at http://pubs.acs.org.

JA021071W